이학박사 학위논문

Neural Activity of Monkey Primary Visual Cortex During Visual Discrimination of Tens-of-milliseconds interval

수십분의 일초 시간의 시각변별 과제에서 원숭이 일차시각피질의 신경 활동

2017 년 2 월

서울대학교 대학원

협동과정 인지과학 전공

윤 태 환

Neural Activity of Monkey Primary Visual Cortex During Visual Discrimination of Tens-of-milliseconds interval

지도 교수 이 춘 길

이 논문을 이학박사 학위논문으로 제출함
2016년 12월

서울대학교 대학원
협동과정 인지과학 전공
윤 태 환

윤태환의 이학박사 학위논문을 인준함
2016년 12월

위 원 장 이 경 민 (인)

부위원장 이 춘 길 (인)

위 원 이 인 아 (인)

위 원 정 민 환 (인)

위 원 이 준 열 (인)

Abstract

Taehwan Yoon

Interdisciplinary Program in Cognitive Science

The Graduate School

Seoul National University

Timing is a fundamental process to represent and discriminate events such as visual motion. However, little is known about precise mechanisms of how tens-of-milliseconds interval, critical for perceiving visual motion (Burt and Sperling 1981), is timed in the mammalian brain (Mauk and Buonomano 2004).

Here we show that the neurons of rhesus primary visual cortex (V1) are sensitive to the temporal interval of tens-of-milliseconds between two stationary visual stimuli that sequentially appeared, the first outside the classical receptive field and the second within the center of receptive field. We further show that while monkeys discriminated the temporal interval, V1 neurons showed two other activity components: one that varied with upcoming choice between interval alternatives with a choice probability that was as strong as reported for orientation discrimination (Nienborg and Cumming 2014), and another activity component in the form of LFP that was related to reward. These results indicate that V1 neurons are sensitive to tens-of-milliseconds interval and modulate their activity according to perceptual decision on temporal interval regardless of physical interval. These results suggest a new role of the

center-surround interaction for interval timing and discrimination.

Keywords : primary visual cortex, interval timing, single cell recording, local field potential, choice probability, monkey

Student Number : 2006-30743

Contents

Figures

1. Introduction

Primates process temporal information over a wide range of scale, from microsecond processing of sound localization to circadian rhythms. For sensory and motor processing such as motion perception or guitar playing, the brain is thought to process time in the range of tens to hundreds of milliseconds. However, the neural mechanisms by which the brain processes the temporal scale of this range are least understood (Mauk and Buonomano, 2004).

In the current study, we examined whether single neurons in the macaque primary visual cortex (V1) were sensitive to tens-of-milliseconds interval between two visual events and how V1 neurons responded during a behavioral task in which the temporal interval was discriminated. Visual events are first broken down into local signals by retinal cells, and these signals are integrated by the central visual system. The primary visual cortex (V1) is the first stage of cortical information processing and shows a dynamic contextual modulation in which the spike activity evoked by the stimulus presented in the receptive field (RF) is modulated by the stimulus presented outside the RF. This so-called surround interaction is important for signal integration because it enhances the selectivity of the neural response by making the integration process more precise. Thus, the spike activity at V1 is more selective and reliable in response to wide-field scenes than to the small stimulus limited to RF.

The rationale of the current study is illustrated in Figure 1. By presenting

the first of the two stimuli at a fixed location outside the RF and the second stimulus at a fixed location within the RF with a variable temporal interval of 30, 50, or 70 ms. The subjects were required to discriminate the three intervals dictated with a two-alternative forced choice in order to get fluid rewards.

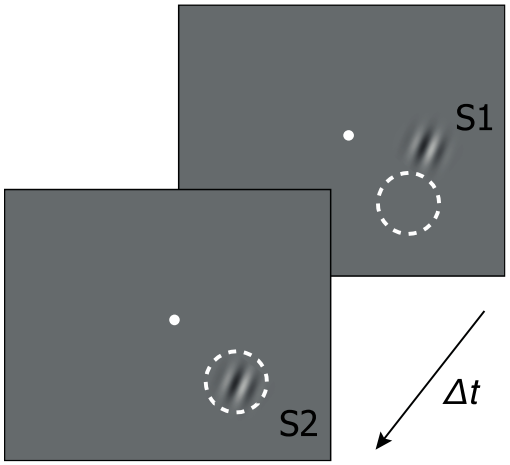

Figure 1. Rationale of experimental design. White dot indicates a fixation stimulus at the center of a computer screen that subject is facing. Dashed white circle represents the classical receptive field (RF) of the cell under study (invisible to the animal). A static Gabor stimulus, designated as S1, appears first outside the RF, and after a temporal delay another static Gabor stimulus (S2) identical to S1 appears next at the RF. The spatiotemporal structure of the S1-S2 stimulus sequence is based on the spatial distance between the two stimuli and on the temporal interval between the onsets of the two stimuli (Δt), or stimulus onset asynchrony (SOA). This is basically an experimental condition of so-called surround interaction in which neural response to the RF stimulus is modulated by a stimulus that appears in the RF surround, but with a temporal interval. We ask in this condition whether the modulation of neural activity of monkey V1 is observed during a behavioral task in which a temporal interval is discriminated, and if so, whether the activity modulation is indeed correlated with behavioral discrimination.

We previously described that in the condition of Figure 1, the spike activity of monkey V1 neurons was modulated by the SOA (Kim et al., 2012). A focal visual stimulus outside the classical receptive field (RF) of a V1 neuron, as in Figure 1, does not evoke a spike response by itself, but evokes changes in the local field potential (LFP). In the condition of Figure 1, the modulation of S2-evoked spike response was dominantly facilitative and was correlated with the change in LFP amplitude, which was pronounced for the cells recorded in the upper cortical layers (Kim et al., 2015).

In the current study, we ask in the condition of Figure 1 whether the modulation of neural activity of monkey V1 is observed during a behavioral task in which the temporal interval is discriminated, and if so, whether the activity modulation is indeed correlated with behavioral discrimination.

1.1. Purpose of the study

The main goal of this study was to examine the reality of interval-related activity component at single neuron in the primary visual cortex (V1) in the perceptually learned animals in the brief interval (30-70 ms) discrimination. Furthermore, we investigated whether interval-related activity component is related to animal behavior through the relationship between neuronal activity and animal decision.

During the study of thesis, two neural activities were analyzed and interpreted, and each signal might reflect different cortical processes, so that we might infer the characteristics cortical process of activity related to each interval and choice. While investigating precisely neural activity properties, eventually, signals related to rewards was examined beyond immediate trial.

The result of the study is purposely to provide evidence of timed-manner processing in V1, and insight for the functional role of V1 during the behavioral task which need temporal processing.

2. Method

2.1. Animal preparation

2.1.1. Subject

Two adult monkeys (DC, NB) participated in this experiment. Both animals were male (Maccaca mulatta), DC was 8.5 years old and NB was 12. All the experimental procedures were under the approval of the Seoul National University Animal Care and Use Committee. During the experiment, the monkeys were housed in the hepa-filtered air circulation colony maintained at 50-60% of humidity and 25 ° C of temperature.

2.1.2. Subject training

Animals were trained to discriminate the ‘Long’ and ‘Short’ interval of two Gabor stimulation presentations. The animals placed in the monkey chair with their heads restrained in the recording room received a juice reward while performing the training stimulation presented on the front monitor. The long interval SOA decreased from 300 ms to 70 ms in the interval length as reinforcement learning was progressed, and the short SOA was fixed at 30 ms interval. SOA 50 ms was not presented before the animals had sufficiently distinguished between SOA 30 ms and 70 ms during the training period.

Two animals showed very different performance records from training. In the case of DC, it seemed to recognize the purpose of the task from the first day of training, and after two weeks, the performance exceeded 75% success rate. NB, however, had less performance and did not reach DC performance until the end of the experiment.

2.1.3. Dura cleaning

A day before the recording session, a dura cleaning was performed. Removal of the brain tissue at the site where a small piece of skull in the recording chamber is removed. Carefully thinning the dura mater at the site where the electrode penetrates will prevent the electrode from breaking or being blocked by the dura mater when performing the actual experiment. Dumont forcep was used for tissue removal and thinning of the Dura mater area with care. During this, animals should be sedated with shallow sedation using ketamine injection and recording was performed in the next day after monkeys' complete awake.

2.2. Experimental setups

2.2.1. Stimulus generation

Visual stimuli were presented on a 24-inch flat CRT monitor (Sony GDM-

FW900, 413 mm x 310 mm) with 800 x 600 pixel resolution. Refresh rate was 100 Hz, Brightness was adjusted to 0, and contrast level to 80 with ODC (On-display control). Viewing distance was 77.6 cm from the animal eye to the center of the screen. At this distance, the screen had a horizontal width of -13.1 to 13.1 degrees and a vertical width of -11.9 to 10.5 degrees. The stimulus presentation computer (master) had two screen outputs. One was the screen presented to the animal and the other was to control the experimental paradigm. Only the stimulus screen was presented to the animal and the researcher monitored both screens outside the recording room. The stimulus was generated by a program written in Matlab (The Mathworks Inc.) and the Psychophysics toolbox.

The second computer (slave) was used for data storage and display. The slave was controlled by the master computer and data acquisition card stored the amplified / filtered analog signal (eye signal, spike activity, LFP, photodiode input) into digitized forms and displayed it on the monitor in real time with experimental status display.

Event onset time was measured more precisely using photodiode (GaAsP, G1115, 410-690 nm, Hamamatsu photonics, Japan). This was attached to the left edge of the computer screen to record such as stimulus onset and juice reward onset/offset timing. Erroneous temporal gap that could occur when the computer monitor screen was refreshed was checked.

2.2.2. Eye monitoring

An infrared video camera (Eye tracking system, ET-49B, Thomas recording, Germany) was used to monitor the horizontal and vertical position of the eye. The eye signals of the camera were input to the DAQ card (NI-DAQ PCI-6013, NI instrument Inc.), sampled and digitized at 500 Hz, and then loaded into Matlab (the Mathworks, Inc.)

The voltage signal of the eye camera was converted to a visual angle based on the fixation point of the screen. Calibration was performed prior to the main experiment to determine the eye position. This was done in two steps, a pursuit and a fixation routine, to extract the gain and offset to convert the voltage signal to an angle value.

In a pursuit routine, moving the stimulus at a constant rate along the horizontal or vertical axis, the juice reward was given using the button when a monkey followed it well. In the case of a less adaptive monkey in a laboratory environment, when a stationary stimulus was presented on the screen to stabilize the gaze, it tended to move the eye distractively rather than along the point, where the moving stimulus made the monkey's attention attracted easier. As the stimulus moved along the horizontal axis (horizontal -10 to +10 degrees, vertical 0 degree), the vertical signal of the eye remained almost constant. The horizontal signal of the eye was also maintained while the stimulus moved along the vertical axis (vertical -5 to +10 degrees, horizontal 0 degree). Therefore, we were able to obtain vertical(d) and horizontal(a) offset, respectively. After tracking, the horizontal or vertical eye position was

displayed to adjust the gain (a or c) to match the pursuit gain to unity.

$$H_{degree} = a \times H_{voltage} + b$$

$$V_{degree} = c \times V_{voltage} + d$$

In fixation routine, the gain and offset were further adjusted with visually guided saccade. The same stimuli were presented at predetermined positions along the horizontal axis (-10, -5, 0, 5, 10) or along the vertical axis (-5, 0, 5) sequentially at 1 second intervals. The monkeys were trained to follow the target position and received a juice reward when the eye reached the target position within the specified window (0.5 - 2 degree). Both target and eye positions were displayed on the computer monitor, and at the point where the eye was fixed at the target position, the offset was calibrated by pressing the key. The relationship between the eye voltage signal and the angular gaze direction was assumed to be linear as shown below, and calibration was completed once offset and gain were determined.

$$\text{Eye Position (degree)} = (\text{Signal}_{voltage} + \text{offset}) \times \text{gain}$$

2.2.3. Neural recording

Extracellular unit recording was performed in the primary visual cortex (V1) of the monkey. In each experiment, two platinum-iridium microelectrodes insulated with quartz (ES12ecpg, Thomas recording, Germany) with a 5-

channel minidrive (MM05, Thomas recording, Germany) were used for each recording session. The diameter of the electrode with the quartz insulator was 80 ㎛ and the spacing between the electrodes according to the guide tube attached to the tip of the Minidrive was 305 ㎛. The range of impedance of electrodes were 1 – 4 ㏁ at 1 KHz. During the recording session, the animals were placed on a monkey chair (Primate Products, USA) and their head was restrained. After the animal was in place properly, the Teflon cap was removed from the recording chamber and the chamber was cleaned with saline solution. The microelectrodes attached to the minidrive was mounted to the chamber and the guide tube was lowered using a micromanipulator to the surface of the dura. Melted agarose (Agarose LE, SeMatrix, Korea, 1.5% saline), which was cooled to 37 ℃, was applied to the around the guide tube in the chamber to stabilize the electrode to prevent noise due to mechanical movement. The juice tube was adjusted to be placed in front of the mouth of the animal and the animal was allowed to lick juice drops when the reward was given. The Minidrive was able to move the electrodes in 0.1 μm steps, independently. Neural activity was amplified 20 times through a preamplifier (em112 / R, Thomas recording, Germany) and diverted to record spike and Local field potential (LFP) activity after passing through the main amplifier (MAF-05, gain: 250-1000). For spike unit extraction, 500 Hz to 20 KHz bandpass filtering was performed using a single unit activity filter (SUA-01, Thomas recording, Germany) and LFP activity was measured using a 5-channel LFP filter (Thomas recording, Germany) with 0.1 – 140 Hz lowpass bandwidth. The amplified neural signals

were digitized at 25 KHz sampling rate and 16-bit resolution DAQ card (PCI-6502E, National Instruments) and simultaneously monitored and stored in real time at computer. Both spike and LFP signals were down-sampled to 1KHz before analysis. In order to help place electrodes in proper position to find the cell, the spike signal was simultaneously displayed on the oscilloscope (Hitachi, VC-6535) and connected to the speaker to let researchers check spike's popping sound. The first cell activity was usually found under 200 - 1800 ㎛ from the point where the guide tube touched the dura.

2.3. Experimental procedure

2.3.1. Experimental Paradigm

In the main behavioral task, monkeys were required to fixate on a central target and discriminate the stimulus onset asynchrony (SOA) between two stationary Gabor stimuli of a high contrast (100%) on a gray background with a mean luminance of 8.65cd/m² (Figure 2). Each trial began with a tone of 800Hz for 100 ms, and two saccade targets representing two choice alternatives, 'Short' (green) and 'Long' (red) intervals, were simultaneously presented for 300 ms to inform the animal of saccade goals in advance. After continuous fixation on a central target for 600, 700, or 800 ms, a stimulus sequence of S1 and S2, each lasting for 20 ms, was presented with an SOA of 30, 50, or 70 ms. Given the spatial distance between S1 and S2, the SOAs translate to the speeds

within a physiological range (Maunsell and Van Essen, 1983). By convention, S1 was first presented at a fixed location outside the RF, and S2 was subsequently presented over the RF. The location of S1 was at a flank zone of the RF and its orientation was collinear to S2. Otherwise, S1 and S2 were identical. The sequence stimulus was presented while the animal maintained the central fixation. When the eye position crossed a circular window of 1.5 deg in diameter centered on the fixation target, the trial was aborted, and a new one started. With additional fixation of 600, 700, or 800 ms after presentation of the sequence stimulus, the fixation target went off and at the same time the two saccade targets came on again. Two conditions for saccade target arrangement, ‘a’ and ‘b’ (Figure 12A) were randomly interleaved, to control the effects of saccade direction, if any, on choice-related neural discharges.

In some trials, S1 or S2 was presented alone, and no saccade targets were presented. The trials of S1-alone were used to evaluate whether S1 was indeed outside the RF. The neural activity in the trials of S2-alone was used as a reference against which the neural activity evoked by the S1-S2 sequence was compared. The trials with S1-S2 sequence with the SOA of 30, 50, or 70 ms are referred to as S30, S50, and S70 throughout the text. The five trial types, S1-alone, S2-alone, S30, S50, and S70, were randomly interleaved within a block, so the animal had no prior anticipation of stimulus condition. The proportion of each sequence condition was made 2-6 times that of S1 or S2 alone.

A liquid reward was delivered after fixation of 200 ms on one of two saccade targets after the eye position entered a circular window of 2 deg in diameter centered on the saccade target. Animals were rewarded for making

saccades to the red target (‘Long’) in the S70, or to the green (‘Short’) in the S30. A straight-left saccade from central fixation was associated with the ‘Short’ in the target arrangement condition ‘a’, whereas the saccade of the same direction and amplitude was associated with the ‘Long’ in the condition ‘b’ (Figure 12A). In the S50, reward was delivered in a randomly-chosen half of trials, irrespective of the animal’s target choice. Monkey NB was sometimes demotivated in the S50, and if so, the relative proportion of the S50 was reduced. The chosen target was made remained on for the rest of trial to help maintain animal’s fixation, and the other target was extinguished.

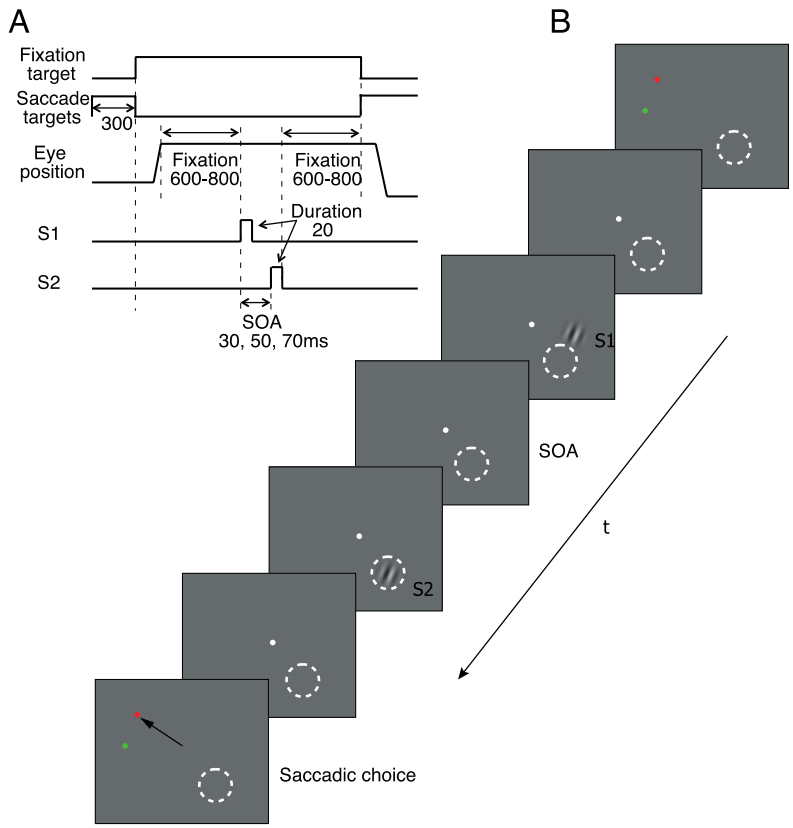

Figure 2. Experimental paradigm. (A) Temporal sequence of a trial. (B) White cross indicates central fixation and a dashed white circle (invisible to the animal) represents the boundary of the classical receptive field (RF). A trial began with a beep sound and two saccade targets (red and green dot) presented for 300 ms. After a fixation duration between 600-800 ms, a static Gabor stimulus appeared outside the RF (S1), and then at the RF (S2) with a stimulus onset asynchrony (SOA) of 30, 50, or 70 ms. The duration of each stimulus was 20 ms. After additional fixation of 600-800 ms, the central fixation target went off and the two saccade targets appeared again. After a successful saccade to and subsequent fixation for 200 ms on the correct target, juice reward was delivered to an animal. The chosen target was maintained on until the end of trial and the unchosen one went off right after the eye landed on the chosen.

2.3.2. Receptive field mapping

Before running the main experiment, we characterized the receptive field properties and determine a stimulus that evoked the maximal response. In this process, a cosine moving grating was used to find the RF position. After roughly finding the location of the RF, we characterized the RF by randomly presenting the various Gabor patch in the dimension such as position, diameter, spatial frequency, phase and orientation. When the position is approximated, a flickering cosine grating was randomly presented for 200 ms while the animal was fixating the eye at the central point. This was repeated 5 to 6 times.

After flickering ended, trials of spike activities in the same stimulus dimension were compiled and aligned with the stimulus onset time. Spike raster and spike density function in peristimulus time period (-100 ~ 400 ms) were computed on-line. Spike counts during the 50 to 200 ms interval after the stimulus onset time were averaged and the magnitude of the mean firing rate was given for each stimulus condition. The tuning curve was obtained by fitting the mean firing rates according to the variable of the condition with DoG (Difference-of-Gaussian). Then, the optimal stimulus condition value is obtained at the peak position of the tuning curve. The mapping process was performed in order of orientation, position, spatial frequency and diameter of the stimulus.

1 dimension:

$$DoG_1(x) = k_1 \times \exp\left(\frac{-(x-c)^2}{2\sigma_1^2}\right) - k_2 \times \exp\left(\frac{-(x-c)^2}{2\sigma_2^2}\right) + l$$

2 dimension:

$$DoG_2(x,y) = \left\{k_{x1} \times \exp\left(\frac{-(x-c_x)^2}{2\sigma_{x1}^2}\right) - k_{x2} \times \exp\left(\frac{-(x-c_x)^2}{2\sigma_{x2}^2}\right)\right\} \times \left\{k_{y1} \times \exp\left(\frac{-(y-c_y)^2}{2\sigma_{y1}^2}\right) - k_{y2} \times \exp\left(\frac{-(y-c_y)^2}{2\sigma_{y2}^2}\right)\right\} + l$$

During the process of mapping the stimulus diameter, the diameter of the Gabor stimuli was randomly presented at the RF center with a 0.2 ° step size. Although the diameter of the maximum activity was determined as the RF diameter, the RF size was set so that the RF diameter did not become as small as possible. The reason for this was that since S1 stimulus would be given adjacent to the boundary of the RF stimulus, if the RF was set small, S1 would invade the RF. At the end of the receptive field mapping, the animals started the main experiment.

2.4. Data Analysis

2.4.1. Spike extraction

Waveforms of spikes were extracted and sorted on-line with spike duration and amplitude and used to quantitatively determine the receptive field (RF) properties. More rigorous sorting was performed off-line to characterize single unit activity quantitatively. In off-line analysis, the spikes were extracted by several criteria in raw data. Firstly, the order of polarity of the peak value of the spike was specified. If the peak values were within a certain range after determining the local maximum and local minimum values in the raw data, they were designated as spike candidates. The Spike candidate set followed the following options as shown below.

Upper threshold

When local maximum is between designated constant values

Lower threshold

When local minimum is between designated constant values

Peak-to-peak height

When peak-to-peak voltage is between constant values

Peak-to-peak interval

When peak-to-peak interval is between constant values

Even when neurons did not produce spikes, high and low potential thresholds were needed to set to prevent artifacts that were above noise levels. The peak to peak interval of the candidate spike's potential should not be greater than 0.4 ms, and then we stored timing and waveform of the spike for sorting process in later. Since it takes about 1 ms to generate one spike, more than 25 data points at 25 KHz sampling rate must be collected to form one spike waveform. In this experiment, one spike waveform was stored at a total of 30 points as 12 points before the first peak and 17 points thereafter.

2.4.2 Spike sorting

The stored waveforms were sorted by the methods based on principal component analysis and K-means clustering. Sorting algorithm (Wavesorter) written in Matlab (the Mathworks, Inc) that was developed in our lab was used. First, 1000 ~ 2000 waveforms were randomly selected and the principal component axes were calculated to account for the largest portion of the variance. When a scatter plot is drawn on a newly constructed axis, similar shapes of waveforms are gathered together to form a cluster. The number of clusters is determined by the Maximum Likelihood Estimation method within a certain range set by the experimenter. Once the centroid values of the clusters were determined, the entire waveforms were classified based on the centroid values. Since the waveforms generated by noise might be included in each group unless the separation was good enough, outlying waveforms those distance from centroid were greater than n times the standard deviation were

removed.

Since the waveform of units could vary with time, clusters could be single unit even if they were divided into different clusters. To confirm this, each cluster was plotted with raster, and the clusters showing clearly similar activity patterns but ones was replaced by the other gradually within a session were integrated into one unit.

Lastly, autocorrelogram was checked to determine whether the characteristics of the inter-spike interval corresponded to the single unit.

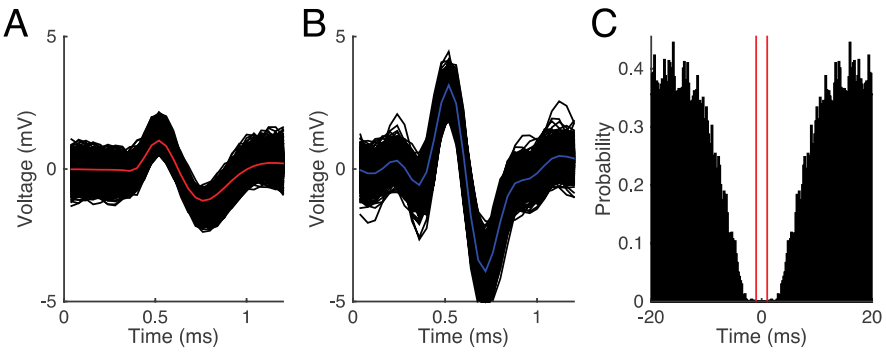

Figure 3. Identification example of single unit. (A,B) Two waveforms grouped by the sorting process. The range of x-axis is 1.2 ms corresponding to 30 points from a sampling rate of 25 KHz. (C) Autocorrelogram of one unit. Bin widh, 1ms. The y-axis indicates probability where bin counts were divided by the number of spikes in the train. Each of two vertical red lines indicates 1 ms lag.

2.4.3 Spike Density function

The spike density function can be obtained by converting the single unit activity classified in the above into a type of binary spike train coding 1 at the spike occurrence time and 0 at the other time point, and then convolution with a specific kernel function. In this study, the growth-decay exponential function, which resembles postsynaptic potential, was used as a kernel. This has the advantage of less distortion of the activity onset point compared to the widely used Gaussian kernel (Thompson et al., 1996). The shape of the growth-decay exponential function *A(t)* is determined by the time constants τg and τd that reflect the growth phase and the decay phase. They were set to 1 ms and 20 ms, respectively, based on the previous physiological studies (Sayer, Friedlander, & Redman, 1990). *k* is a constant for the area under kernel to be a unity.

$$\mathrm{A(t)} = \left(1 - \exp\left(-\frac{t}{\tau_g}\right)\right) \times \exp\left(-\frac{t}{\tau_d}\right) \times k$$

2.4.4 Validation of data

Invalid trials were removed by off-line analysis. Unsteady fixation, trials with multiple saccades toward the saccade target or a saccade with latency longer than 600 ms, trials with the velocity of eye outlying 2 SDs from the average around S2 onset (from -80 to 20 ms of S2 onset), trials with the firing rate during the visual response (from 50 to 150 ms of S2 onset) exceeding 3

SDs from the mean , trials with S1 alone activity exceeding 5 % of S2 alone activity due to encroaching of S1 into RF, trials with LFP that saturated into positive or negative extremes due to sudden noise were excluded.

2.4.5 Spectrogram

For spectral power component analysis of LFP activity for each cell, a spectrogram was calculated using the 'Chronux' (see detail functional descriptions in Chronux.org) that provides LFP spectral analysis toolbox. The multi-taper time-frequency spectrum function for continuous process was used for this analysis. The sampling frequency of the input data was set to 1 KHz, the pass band was set to 0 - 140 Hz, the taper parameter was set to [2 3], the moving time window was set to 250 ms, and the moving step was set to 1 ms.

2.4.6. Distance Index

In order to quantify the difference in spike density across two or three stimulus conditions, we defined distance index, *DI(t)* for each cell, as following:

$$D(t) = \sum_{i=1}^{N} \sum_{j=1}^{N} \left| r_i(t) - r_j(t) \right| / 2$$

$$DI(t) = \frac{D(t) - M_D(t)}{S_D(t)}$$

where $r_i(t)$ and $r_j(t)$ are instantaneous spike densities averaged over all trials for *i* and *j* stimulus conditions. We defined a distance measure *D(t)* summing the differences in mean spike density over the period from *t-5 ms* to *t+5 ms* between possible pairs of conditions, $r_i(t)$ and $r_j(t)$. *D(t)* was calculated every 1 ms. We evaluated statistical significance of *D(t)* with a permutation test in which simulation under the hypothesis of no effects of stimulus condition was repeated 100,000 times to derive a probability distribution of *D(t)* every 1 ms. The statistical significance of *D(t)* was controlled for false discovery due to multiple comparison (Hochberg and Benjamini, 1990). Then, a standardized distance measure, *DI(t)*, was calculated by subtracting the mean of 100,000 simulated *D(t),* $M_D(t)$, and divided by the standard deviation of 100,000 simulated *D(t)* based on randomly-shuffled trials, $S_D(t)$. Figure 4 shows one example unit (Figure 8) for the statistical test that was performed in population summary data (Figure 9). Note that the significant duration where real distance outlies from the resampled distribution of distances.

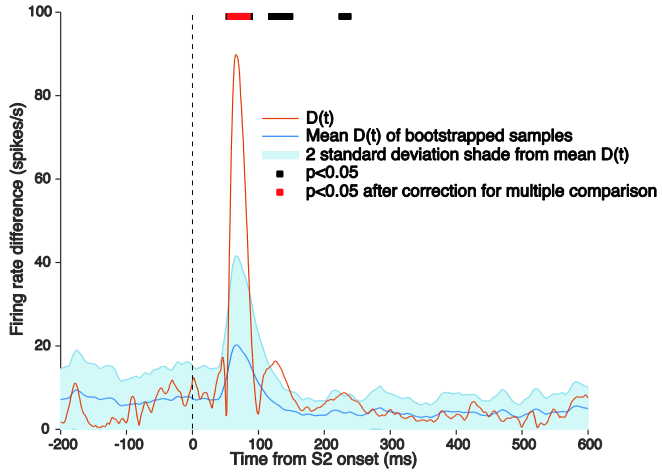

Figure 4. Distance index metric. This illustrates the procedures for computation of the distance, distance index and its permutation test with the data obtained from one example recording session. D(t) is an actual difference in spike density among stimulus conditions measured every 1 ms (red trace). Bootstrap mean (blue trace) is the average distance from a simulated distribution prepared by resampling 100,000 times. Shade shows 2 SD boundary of distance distribution at each time point. When D(t) exceeded the 2 SD boundary we took those time points as a candidate significant times (black bar above the traces). Statistical significance was corrected for multiple comparison (Hochberg and Benjamin, 1990), after which significant time points are indicated red.

2.4.7. Test of eye stability

Since the position of the eye before stimulus presentation can affect the neural activity, we examined the eye position during the period of 20 ms of S2. In terms of Mahalanobis distance, eye positions outlying beyond 2 SDs from the mean were removed.

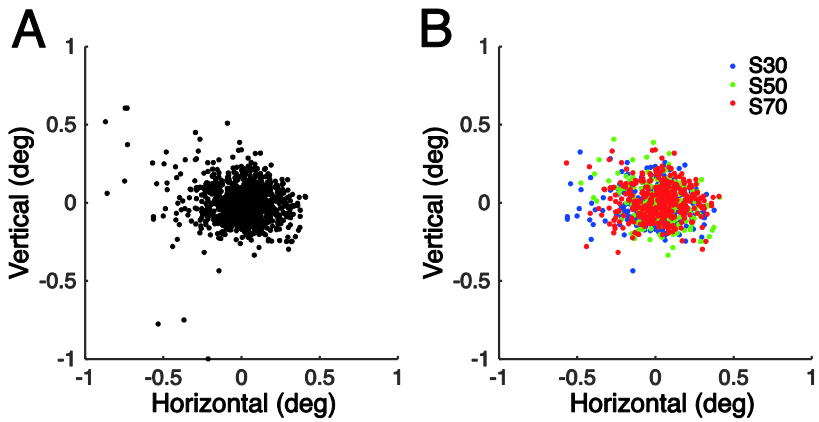

Figure 5. Test of eye stability. (A) Eye position scatter during S2 (20 ms duration) in an example session. (B) Eye position scatter excluding the trials with the eye positions outlying beyond 2 SD based on Mahalanobis distance measure. Eye positions for each of three different SOA conditions are marked with different colors. The horizontal and vertical positions were not statistically different (Kruskal-Wallis test, p=0.54 for the horizontal and p=0.13 for the vertical and similar results for overall population of cells in this experiment.).

2.4.8. Detection of microsaccades.

To detect microsaccades, horizontal and vertical eye position signals were first low-pass filtered (Butterworth, cutoff frequency= 40 Hz), and differentiated for instantaneous horizontal and vertical velocity signals, h and v, and combined for radial velocity, $\sqrt{h^2 + v^2}$. A radial velocity threshold of 10 deg/s was used to localize putative microsaccades and an acceleration threshold of 550 deg/s^2 was used to define their onset and -550 deg/ s^2 for their offset (Hafed et al., 2011). Eye position and velocity traces of each trial were visually inspected and those contaminated from animal's movements were

discarded. Eye movements with amplitude less than 0.05 deg or with the interval from the preceding saccade or microsaccade less than 100 ms were also discarded.

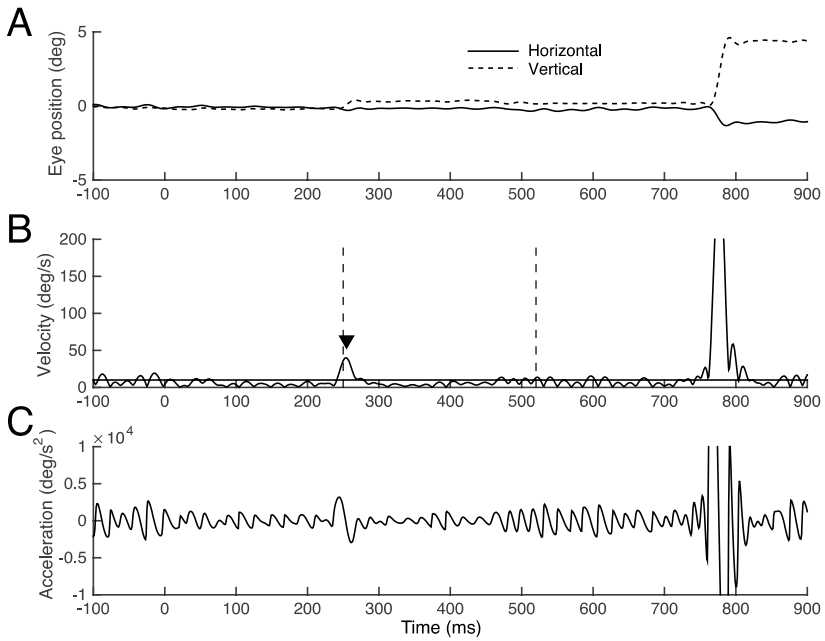

Figure 6. Detection of microsaccades. (A) Horizontal and vertical eye positions are shown during one example session. X-axis indicates time from S2 onset in milliseconds. (B) Radial eye velocity with a threshold of 10 deg/s (horizontal line). Two vertical dashed lines indicate *the late period*, corresponding to 250-520 ms from S2 onset, as will be described in Results. An inverted filled triangle represents a detected microsaccade. (C) Radial eye acceleration to help measure the onset and offset of a microsaccade.

2.4.9 Choice-related activity component period.

Normalized spike density for the analysis, sp_N, was defined as relative ratio of spike density, sp, to mean spike density during the post-stimulus period of 50-150ms of S2 alone condition, s2, both adjusted for mean spontaneous activity level during the period of 200ms before S2 onset, s, sp_N=(sp-s)/(s2-s). To delineate the period of choice-related activity component, we calculated the time course of Pearson product-moment correlation coefficient every 10 ms as following,

$$r(t)_{xy} = \frac{\sum_{i=1}^{n}[x(t)_i - \overline{x(t)}][(y(t)_i - \overline{y(t)}]}{\sqrt{\sum_{i=1}^{n}[x(t)_i - \overline{x(t)}]^2}\sqrt{\sum_{i=1}^{n}[y(t)_i - \overline{y(t)}]^2}}$$

where n=84, $x(t)_i$ is the difference in mean normalized spike density between S30 and S70 conditions, s30(t) and s70(t) during an analysis window of 100ms, $[\int_{t-50}^{t+50} \mathrm{s30}(\tau)d\tau - \int_{t-50}^{t+50} \mathrm{s70}(\tau)d\tau]/100$, and $y(t)_i$ is the difference in mean normalized spike density between 'Short' and 'Long' choice trials of S50 conditions, $\mathrm{s50}_{\mathrm{short}}$ and $\mathrm{s50}_{\mathrm{long}}$, $[\int_{t-50}^{t+50} s50_{short}(\tau)d\tau - \int_{t-50}^{t+50} s50_{long}(\tau)d\tau]/100$. The correlation coefficients were tested for statistical significance with bootstrapping (1000 times) with a function (bootstrp.m) provided by Matlab (The Mathworks, US). The period of significant correlation ($p<0.05$) was defined as choice-related activity component period.

2.4.10. Choice probability

The correlation between single neuron activity and the animal's choice on a trial-to-trial basis was quantified as CP (Britten et al., 1996). For this, trials of S50 were divided into two groups according to the animal's choice, 'Short' and 'Long', and from each of these trials, the mean spike density during the choice-related activity component period (250-520 ms of target onset) was calculated and used. The CP of 0.5 indicates that the two distributions of mean spike density associated with the 'Short' and 'Long' choices are identical, and thus, the neuron's response is uninformative about the animal's choice on each trial. The CP can vary up to 1 that would indicate that the two distributions are non-overlapping, and thus neuron's response is a perfect predictor of animal's choice.

3. Results

3.1. Data Summary

Total 84 valid units out of 122 recorded units from 76 sites in the dorsal operculum of V1 were acquired from two animals.

DC 52 sites, 91 units, 65 valid units

NB 24 sites, 31 units, 19 valid units

In the reward-related activity component analysis, there were a few sessions with a short recording end time of LFP. Therefore, with additional excluded sessions, DC 32 and NB 23 sessions were used in the analysis.

3.2. Behavioral performance in visual discrimination

Two male rhesus monkeys were trained to discriminate the temporal intervals of 30, 50, and 70 ms between two stationary Gabor stimuli, referred to as S1 and S2, that sequentially appeared in periphery. The subjects reported the interval by making a saccadic eye movement to one of two separate color targets representing ‘Short’ and ‘Long’ intervals. A liquid reward was delivered for saccades made toward a green target (‘Short’) in the trials in which the temporal interval was 30 ms, and a red target (‘Long’) when the interval was 70 ms. In the trials in which the interval was 50 ms, the reward was delivered

in randomly chosen half of trials, regardless of animal's choice, and the monkeys split their choices between 'Short' and 'Long'.

Monkey DC learned this task within two weeks reaching to a criterion performance (75% correct rate), whereas monkey NB took months and never reached the performance of DC over the experimental period of six months, as revealed in the overall slope of dashed line.

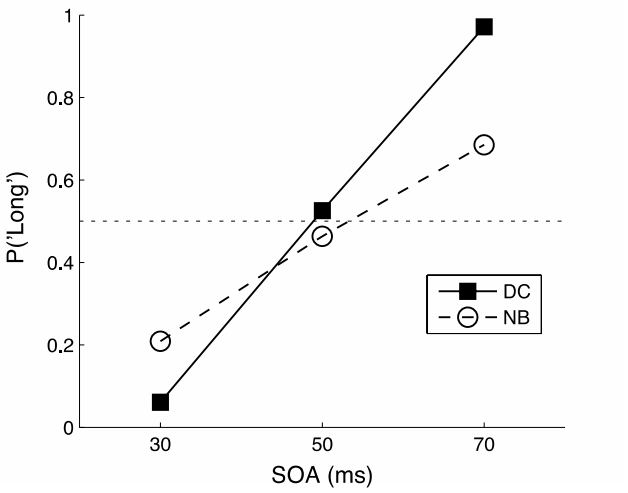

Figure 7. Behavioral performance of two monkeys, DC and NB in representative sessions. Each symbol indicates the probability of choosing the 'Long' target as a function of SOA in the two-alternative forced choice condition. Note that the probability increased with SOA, and for the SOA of 50 ms, the choice was split between 'Long' and 'Short' in both monkeys. Monkey DC learned this task within two weeks reaching to a criterion performance (75% correct rate), whereas monkey NB took months and never reached the performance of DC over the experimental period of six months, as revealed in the overall slope of dashed line.

3.3. Interval-related spike activity component

3.3.1. Example cell activity

Figure 8 illustrates the activity of a single V1 cell during the task. The stimulus was optimal for the cell when it appeared over the RF (dashed circle, Figure 8A), evoking a burst of spike response (Figure 8B). When the identical Gabor stimulus was presented at one flank of the RF along the cell's preferred orientation as indicated as S1 in Figure 8A, it did not evoke a spike response above a criterion level (5% of S2-alone condition) (Figure 8B). Nevertheless, as previous studies on surround interaction have shown (Allman et al., 1985; Series et al., 2003; Angelucci and Bressloff, 2006), the same stimulus (S1) in the receptive field surround modulated the cell's response to the RF stimulus (S2) (Figure 8C). Importantly, the magnitude of this modulation differed according to the temporal interval between the two stimuli. Note that in all trials in Figure 8C optimal stimulus was equally presented over the cell's receptive field. The sequence direction was parallel to the cell's preferred orientation axis in the current study. Many V1 neurons respond to motion in the direction parallel to the spatial orientation of the RF (Geisler et al., 2001). For sequence direction orthogonal to orientation axis also modulate neural activity (Kim et al., 2012).

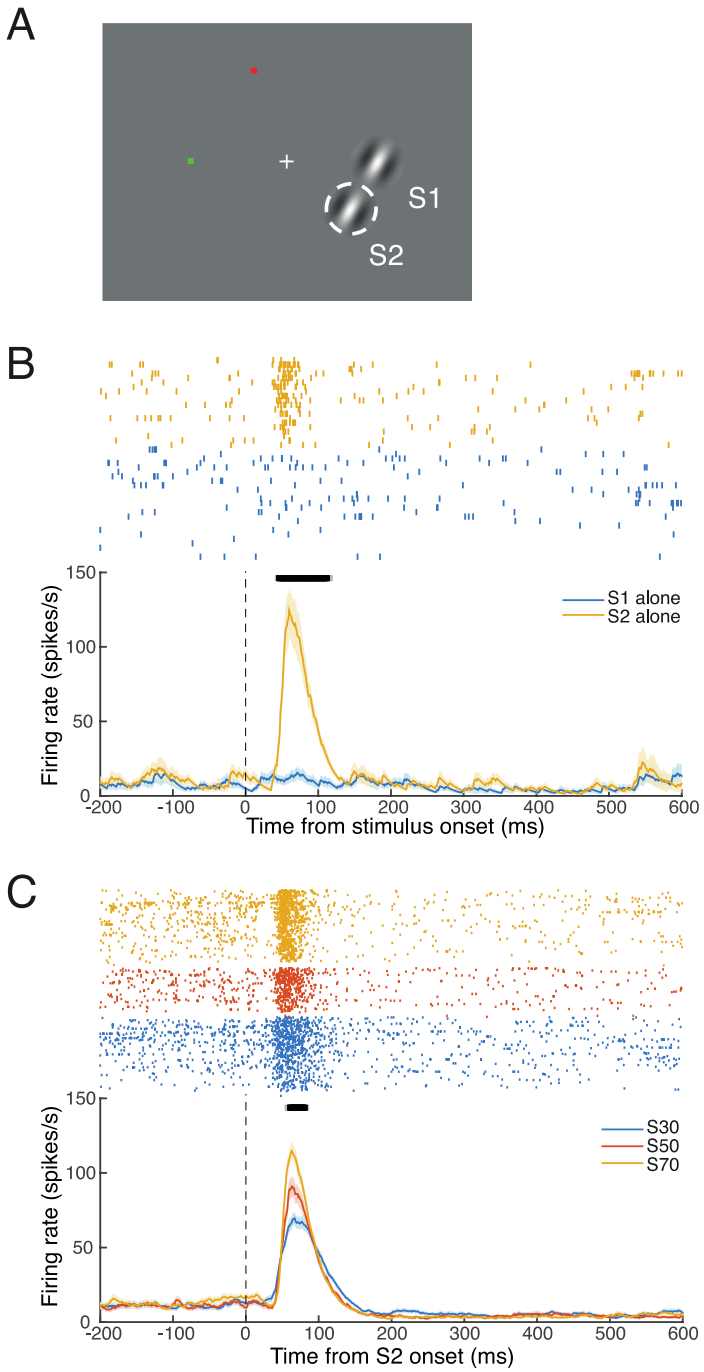

Figure 8. Interval-related activity component of a representative cell (#20130725). (A) Spatial layout of the stimulus configuration tailored for the cell. Cross: position of fixation target; green and red squares (0.19x0.19 deg): saccade targets for 'Short' and 'Long' choices, respectively. Both targets were equidistant (4.25 deg) from the fixation

target in the hemifield opposite to the RF. The RF (dashed circle invisible to animal) was centered 2.8 deg right and 2.2 deg down. An identical stimulus was first presented one RF diameter away from the RF center (S1) and then over the RF (S2), in the direction parallel to the cell's preferred orientation (60°). The optimal spatial frequency was 0.8 cycles/deg. 100% of contrast of Gabor stimuli was used in all experiment. (B) Raster (upper) and mean spike density (lower) plots for S1-alone and S2-alone conditions. S2-alone, but not S1-alone evoked a burst of visual response, indicating that S1 was outside the RF. (C) Raster (upper) and mean spike density (lower) plots of the cell's activity during S1-S2 sequence conditions, sorted according to the SOA, aligned at S2 onset, as indicated as S30, S50, and S70, respectively. Note that the magnitude of spike response was different depending on SOA. The shades of spike density plots of B and C indicate one SE. Horizontal bars at the top of the density plots in B and C indicate the epochs of significant distance (D(t), black: $p<0.01$; gray: $p<0.05$) based on a permutation test performed with correction for multiple comparison. All trial types, S1 alone, S2 alone, and sequence conditions with three intervals were shuffled within a block during the discrimination task.

3.3.2. Population summary

Figure 9 illustrates the time course of interval-related activity component pooled over 84 cells from two monkeys (65 from monkey DC, 19 from monkey NB). The interval-related activity component was observed in two periods, as revealed with the epochs of significant distance index (DI) that quantifies the difference in spike density among stimulus conditions (Figure 9A), or with the mean DI (Figure 10). Overall, approximately 15% of cells showed a significant ($p<0.05$) interval-related activity component during an earlier period (Figure 9A). A significant interval-related activity component was also apparent during a later period, and variably observed across cells (Figure 9A).

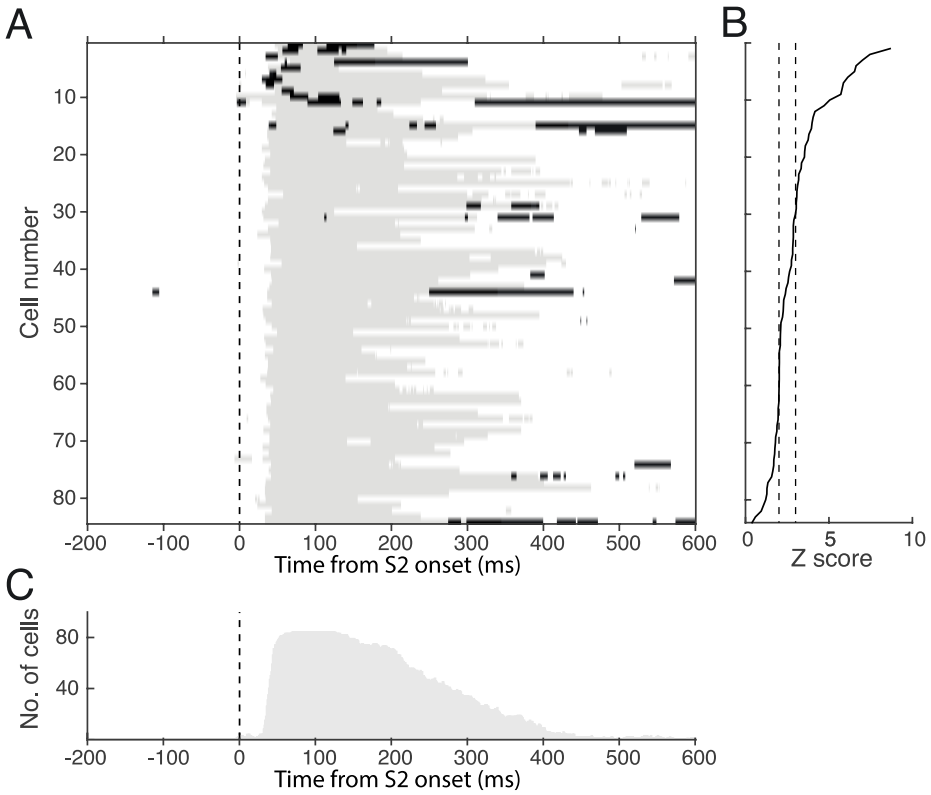

Figure 9. Population summary of interval-related activity component. (A) Epochs of significant difference in distance measure for each cell, *D(t)*, sorted according to its magnitude during 0-150 ms of S2 onset. Significant epochs of D(t) for each cell are shown in black ($p<0.05$) horizontal lines, based on a permutation test and corrected for multiple comparison. Each of gray horizontal lines indicates the duration of visual activity where the mean firing rate of all trials in which S2 was presented at the RF exceeded 5 % of the peak of mean firing rate. (B) Maximum magnitude of *DI(t)* for each cell during 0-150 ms of S2 onset. *DI(t)* is a standardized form of *D(t)* from 100,000 times resampled distribution (see Methods). Cells were sorted based on this magnitude. Two vertical dashed lines indicate 2 and 3 in Z-score. Sixty and twenty-seven cells exceeded 2 SD and 3 SD, respectively. (C) Sum of visual activity duration for all cells, by collapsing gray lines in A.

The interval-related activity component was not due to the difference in eye position; for the example cell of Figure 8, the mean eye position during the S2 presentation of 20 ms for the three SOA conditions clustered within +/-0.4 deg in both horizontal and vertical dimensions and was not different among three conditions (Kruskal-Wallis test, p=0.54 for the horizontal and p=0.13 for the vertical). Similar results were found for overall population of cells; the mean p-values of Kruskal-Wallis test for horizontal and vertical eye positions of monkey DC were 0.50 (±0.29) and 0.43 (±0.28), and those of monkey NB were 0.48 (±0.33) and 0.44 (±0.33), respectively.

The time course of interval-related activity component also showed two periods of high DI, earlier and later (Figure 10). Below, we show that these two periods are related to interval itself and choice, respectively. Two vertical real lines in Figure 10 (250-520 ms) indicate the period with the choice-related signal as determined with a correlation analysis described later. (see 3.5.3.)

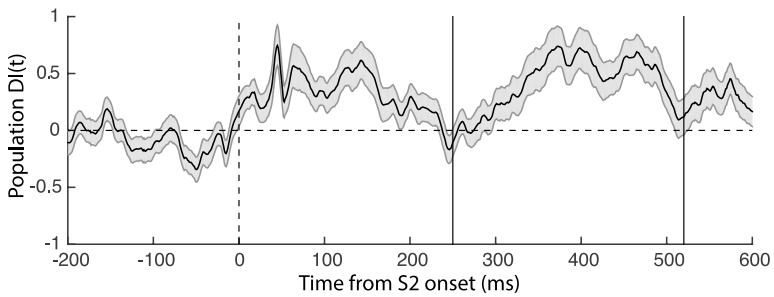

Figure 10. Time course of the population DI(t). Shade indicates 1 SE. Two vertical solid lines indicate *the late period*, i.e. the period of choice-related activity component (see 3.5.3.).

3.3.3. Pattern of interval-related activity component

The differential response across the temporal interval could be due to suppression or facilitation (Kim et al., 2012). The magnitude of activity in response to the RF stimulus alone served a baseline against which the modulatory effect of preceding S1 was evaluated. In the cell of Figure 8, the response magnitude in S70, the largest of three SOA conditions (Figure 8C), was similar to that in S2-alone condition, indicating that the S1 suppressed the neural response to S2 at the SOA of 30 and 50 ms, and that this suppression was greater with the SOA of 30 ms. Of 84 cells recorded from two monkeys, 13 cells (15.5%) showed a significant DI ($p<0.05$) during 50-150 ms after S2 onset, and in 9 of these 13 cells (69.2%), the response was the lowest in S30 condition. In 8 of these 9 cells, the response magnitude in S30 condition was lower than that of S2-alone condition, suggesting a suppressive interaction of S1, as in Figure 8. In four remaining cells out of the above 13 cells with significant DI, the lowest response was observed in S70 (one cell), in S50 (two cells), and equally in S50 and S70 conditions (one cell). Overall, in 39 SOA conditions of the above 13 cells, the response magnitude was lower than in S2-alone condition for 26 cases, and larger for 13 cases. Therefore, the interval-related activity component and its relation to SOA were due dominantly to suppression with the greatest effect in the S30 trials.

3.4. Example of invalid cell

An example cell in Figure 11, S1 alone evoked spike activity (50-150 ms of S2 onset) by exceeding 5 % of that of S2 alone condition (Figure 11B). Therefore, it was discarded for analysis. Note that the activity evoked by S1 systematically (20 ms steps) precedes the main activity evoked by S2, indicating that the manipulation of stimulus timing and SOA was effective (Figure 11C).

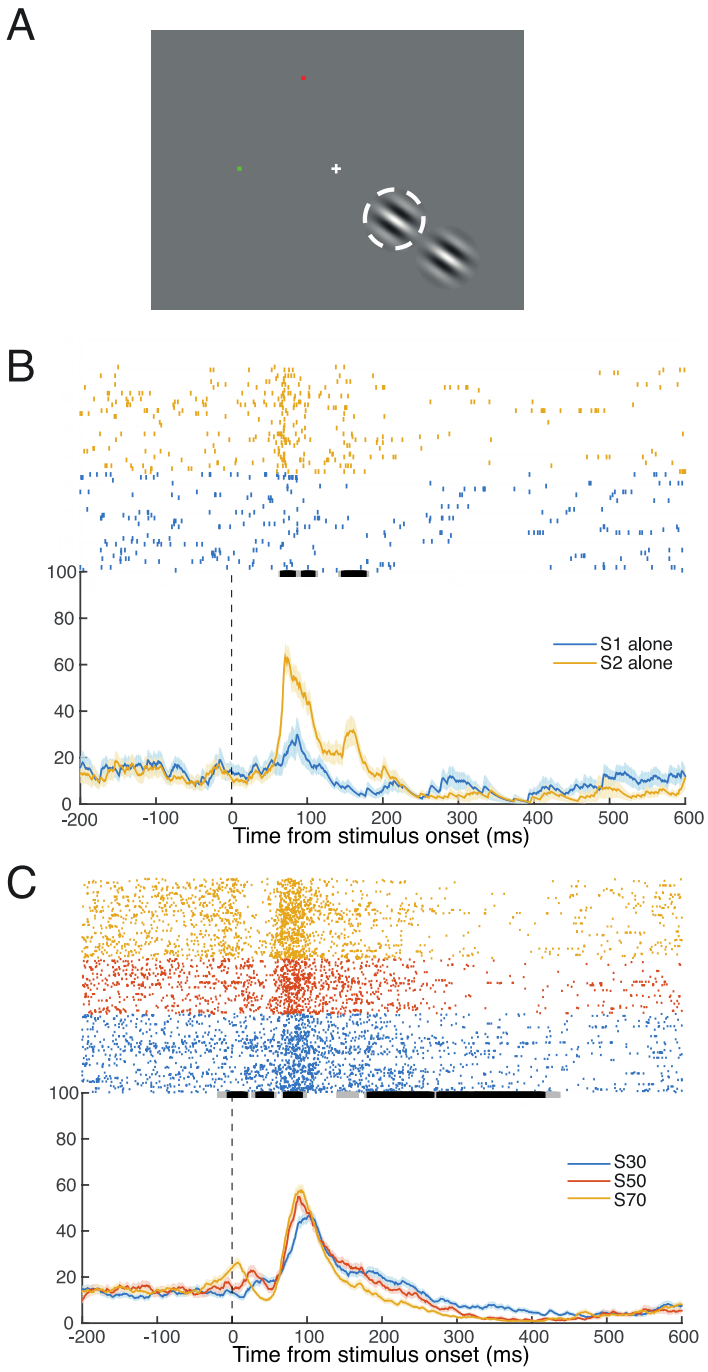

Figure 11. Activity of an example invalid cell (#20130704). Same convention as Figure 8. (A) Spatial layout of the stimulus configuration. The RF was centered at 2.6 deg right and 2.3 deg down. Gabor properties: diameter 2.8 deg, orientation 145 deg, spatial frequency 1.2 cpd. (B) Raster (upper) and mean spike density (lower) plots for S1-alone

and S2-alone conditions. In this cell, S1 alone evoked spike activity (50-150 ms of S2 onset) by exceeding 5 % of that of S2 alone condition. Therefore, it was discarded for analysis. (C) Raster (upper) and mean spike density (lower) plots of the cell's activity during S1-S2 sequence conditions. Significance was not corrected for multiple comparison in B and C.

3.5. Choice-related activity component

3.5.1. Example cell activity

If V1 neurons carry the choice-related signals, their activity is predicted to vary according to animal's choice between the two interval alternatives regardless of SOA. Figure 12 illustrates spike activity of the cell with choice-related activity component. Unlike the cell of Figure 8, the interval-related activity component of this cell was observed during the later period, such that the activity during the S30 condition was relatively higher than that during the S70 condition, and the activity during the S50 was in-between (Figure 12B). The magnitude of activity during the later period depended on whether the upcoming saccade was made to the 'Short' or 'Long' target, even in response to the identical SOA of 50 ms (Figure 12C). The difference in activity was not due to the difference in saccade direction; even when the saccade direction was controlled same (straight left) by using two conditions for saccade target arrangement (Figure 12A), the difference in activity related to the choice was similarly observed (Figure 12D). Microsaccades occasionally occurred during the late period, but the difference in activity was not due to differential

occurrence of microsaccades; the mean numbers of microsaccades counted during the 'choice-related activity component period' (see 3.5.3., defined in 2.4.9.) were 1.11 (±0.56) and 1.14 (±0.66) for 'Short' and 'Long' response trials, respectively, and this difference was not significant (t-test, p=0.45) and results for all cells were similar; mean number of microsaccades were 1.13 (±0.14) and 1.16 (±0.10) for 'Short' and 'Long'. Note in Figure 12C and D that 'Short' choice was associated with a relatively higher activity compared to 'Long' choice, in the direction same as the difference between S30 and S70 in Figure 12B. These results indicate that the activity of the cell during the later period was related to upcoming choice.

It has been known that the activity in the sensory cortex shows signals reflecting perceptual decision apparently provided by top-down connections as well as feedforward signals reflecting stimulus encoding (Britten et al., 1996; Nienborg and Cumming, 2009; Poort et al., 2012). The choice component in our behavioral task may be an indication of top-down processes, or alternatively, it evolves within V1 probably in conjunction with other areas. The cell of Figure 12 suggests the latter. In the S50, animal's choice splits and the variability related to choice appears in early sensory response; a higher activity before 250 ms continues to maintain the activity level of S30 condition during the choice-related activity component period that is correlated to the 'Short' choice, whereas a lower activity before 250 ms leads to the activity level of S70 condition during the choice-related activity component period that is correlated to the 'Long' choice (Figure 12C).

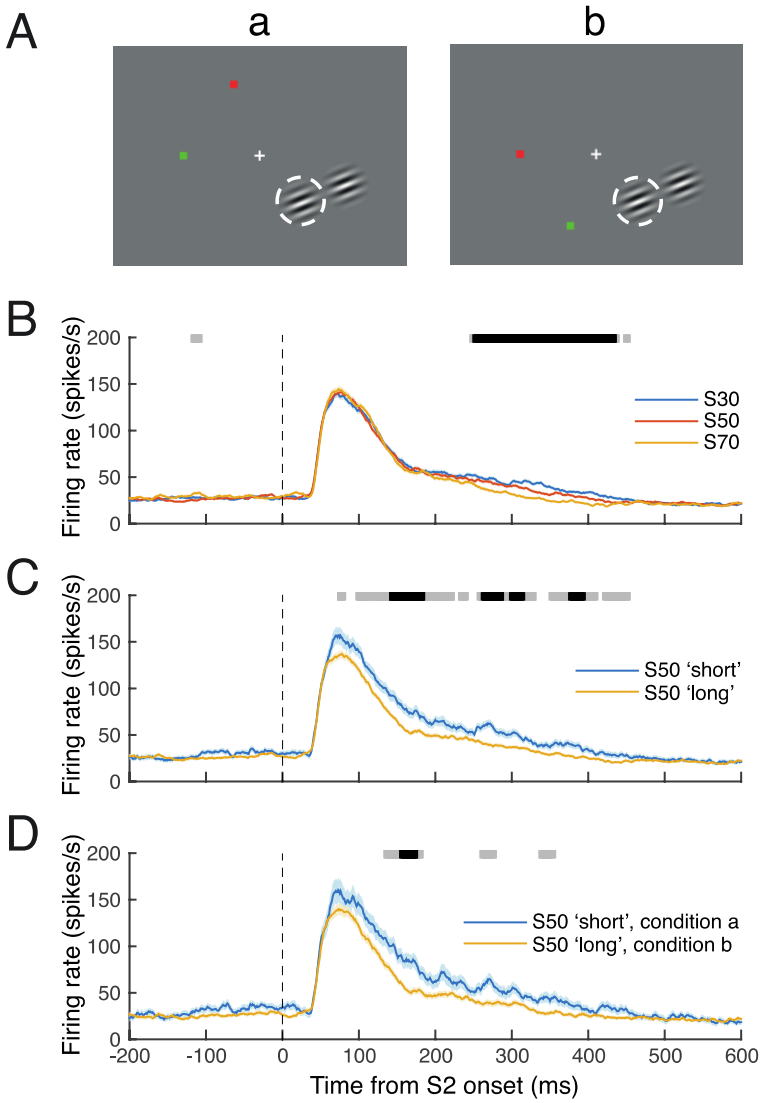

Figure 12. A representative cell with the choice-related activity component (#20100917). (A) Spatial layout of target conditions, a and b. These two conditions were interleaved. Same convention as Figure 8A. The RF was centered at 2.7 deg right and 2.2 deg down. (B) Mean spike density traces of the cell's activity during S1-S2 sequence conditions. (C) Mean spike density traces of S50 trials of Figure 12A divided by animal's choice, 'Short' and 'Long'. (D) Control of saccade direction. Mean spike density trace for the trials of 'Short' choice in the target condition a, and that for 'Long' choice in the condition b. Thus, the saccade target appeared straight left to the fixation point in all these trials. Roughly half of trials shown in C are plotted. Convention of B-D are same as the lower part of Figure 8D. Horizontal bars at the top of the density

plots in B, C and D indicate the epochs of significant distance (D(t), black: $p<0.01$; gray: $p<0.05$) based on a permutation test performed with correction for multiple comparison. The number of trials averaged for each condition is 282 (S30), 291 (S50) and 288 (S70) in B, 73 (S50, 'Short') and 218 (S50, 'Long') in C, and 40 (S50, 'Short', a) and 114 (S50, 'Long', b) in D. A relatively greater number of trials for 'Long' choice suggests either that the animal was biased toward the 'Long' choice or that S50 was perceptually closer to S70 than to S30, and explains differential magnitude of activity variability between choices in C and D (a larger variability in the condition of less trials).

3.5.2. Population summary

Figure 13 illustrates the time course of choice-related activity component pooled over 84 cells from two monkeys. The epochs of significant distance index (DI) that quantifies the difference between split choices ('Short' and 'Long') in spike density in S50 trials (Figure 13A) or with the mean DI (Figure 13C).

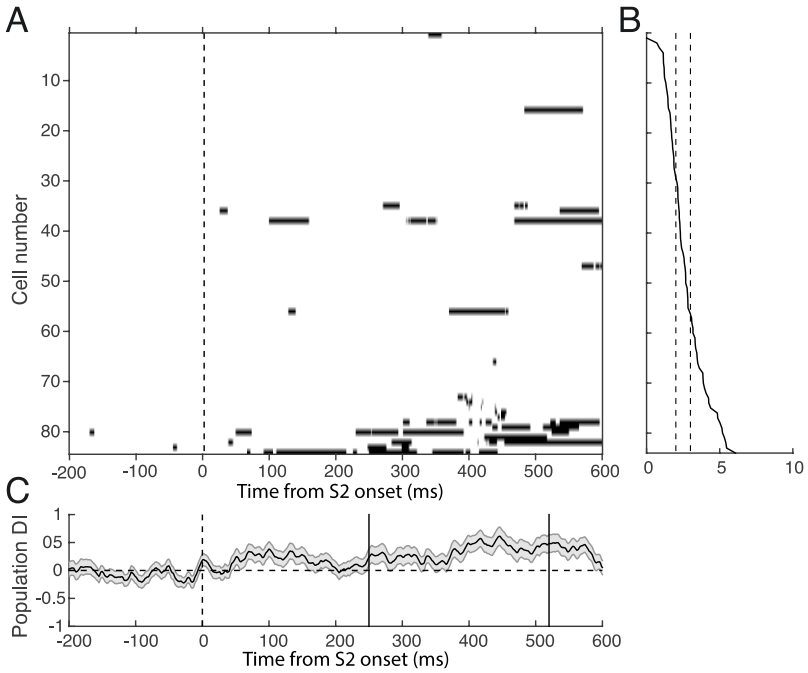

Figure 13. Population summary of the choice-related activity component. (A) The epochs of significant ($p<0.05$) difference between S50 'Short' and S50 'Long' trials in distance measure for each cell. Same convention as Figure 9A, but without the marks of the duration of visual activity. Cells are sorted according to the magnitude of distance measure during 250-520 ms of S2 onset (ascending order). (B) Maximum magnitude of DI(t) for each cell during 250-520 ms of S2 onset. Convention is same as Figure 9B. Fifty-four and twenty-seven cells exceeded 2 SD and 3SD, respectively. (C) Time course of population DI(t). Convention is same as Figure 10.

3.5.3. Period of choice-related activity component

The activity difference between S30 and S70 conditions reflects both interval encoding and choice processes, and that between 'Short' and 'Long' choice trials of S50 condition reflects only the choice process. To delineate the period of choice-related activity component, we calculated the time course of

Pearson product-moment correlation coefficient between the two differences: spike density in S30 minus that in S70 condition and spike density in ‘Short’ trials minus that in ‘Long’ trials of S50 condition. A significant positive correlation coefficient between the two differences would indicate the presence of signal component related to choice, and was observed during 250-520 ms after S2 onset (Figure 14). In other words, when the spike activity in S30 condition was higher (or lower) than in S70 condition during this period, the activity was also higher (or lower) in ‘Short’ trials than in ‘Long’ trials of S50 condition. Based on this, we defined the period of choice-related activity component, as 250-520 ms after S2 onset (Figure 14). The start time of this period agreed well with a break point in the population DI of Figure 10. On the other hand, during the early period, the correlation coefficient was not significantly different from zero (Figure 14). This suggests that the significant DI during 0-250 ms (Figure 10) represents the signal component related to interval. Thus, V1 neurons appear to show both activity components related to interval and choice decision processes in initial sensory and the late periods, respectively.

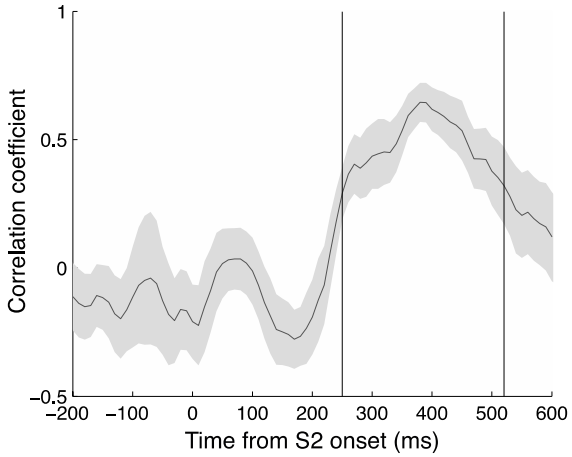

Figure 14. Delineation of *the choice-related activity component* period. Shown is the time course of Pearson product-moment correlation coefficient for 84 cells (see Methods). Only correct trials of S30 and S70 were included for this calculation. Shade indicates ±SE. Significant correlation ($p<0.05$) was observed during the period of 250-520 ms after S2 onset (vertical solid lines).

3.5.4. Absence of the choice-related activity component in late period

The choice-related component diminished well before the 'go' signal (fixation offset) was given (Figures 15B,C). When spike density was aligned at the time of saccadic onset, no significant DI between choices was observed during the presaccadic period of 375 ms in this cell, and for overall cell population, the incidence of significant DI was low during presaccadic period of 300 ms (not shown). This suggests that once the association between the interval and saccadic target on a trial-to-trial basis was completed to which V1 apparently contribute, the related signal is then maintained in areas other than V1 until saccadic onset.

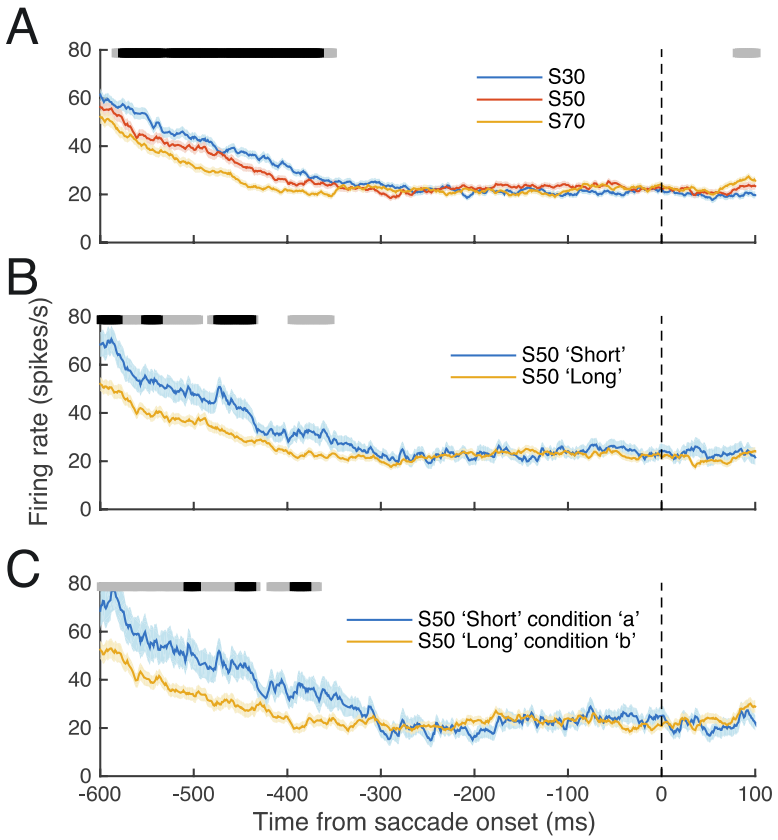

Figure 15. Absence of the choice-related activity component immediately before saccadic choice. Same cell (#20100917) in Figure 12 and convention is the same as Figure 12A-C. (A) Mean spike density traces of the cell's activity during S1-S2 sequence conditions. Traces are aligned to saccade onset time. (B) Mean spike density traces of S50 trials of Figure 15A divided according to animal's choice: 'Short' and 'Long'. (C) Control of saccade direction. Mean spike density trace for the trials of 'Short' choice in the target condition a and that for 'Long' choice in the condition b. (B,C) Choice-related activity component decreased and then disappeared before -375 ms of saccade onset.

It is more likely that V1 participates in generation of decision (as reflected in choice signal), and once decision is completed, choice-related signal evacuates from V1 to other areas for about 300ms until saccade is made. LIP

which is known to be in working memory is a likely structure to hold the choice-related activity component during late period.

3.5.5. Relation between during early and late periods

We examined the relationship between the activity difference during the early and late periods for all cells, by relating the activity difference calculated by subtracting the spike density in 'Long' choice trials from that in 'Short' choice trials in the early period to that of choice-related activity component period. For this purpose, we defined the early period as 50-150 ms after S2 onset that contained the strongest sensory response. The correlation coefficient between the activities during early- and choice-related periods of S50 was 0.62 ($p<10^{-9}$), supporting the possibility that V1 participates in generating the choice-related activity component (Figure 16).

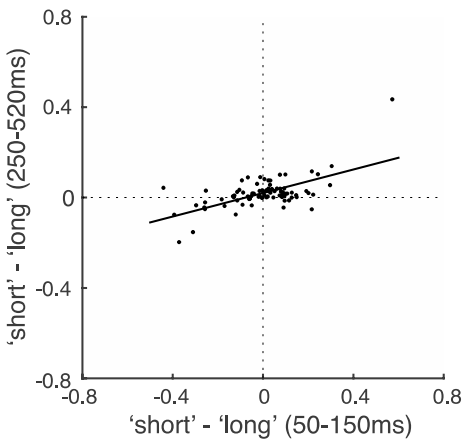

Figure 16. Scatter plot between the neural activities during the early and the late periods.

Each dot represents a cell's normalized activity difference in terms of spike density, calculated by subtracting the mean normalized spike density of 'Long'-chosen trials from that of 'Short'-chosen trials of S50 condition during 50-150 ms of S2 onset (x-axis) and that during the choice-related activity component period, 250-520 ms of S2 onset (y-axis). The linear regression equation is y=0.26x+0.02.

3.5.6. Choice probability

We next examined whether the activity during the choice-related activity component period is indeed related to behavioral choice. For this, we calculated the correlation between trial-to-trial variability of neural activity during choice-related activity component period and behavioral choice. This correlation, known as choice probability (CP), quantifies the difference in the distribution of neural response magnitude between trials leading to one choice or the other (Britten et al., 1996). We defined the choice of 'Short' as a target and that of 'Long' as an alternative in CP analysis. The mean CP of spike activity between 'Short' and 'Long' choices during the choice-related activity component period of S50, i.e., in the identical stimulus condition, was 0.53, and 20 of 84 cells (23.81%) showed statistically significant CPs ($p<0.05$, black bars, Figure 17). Note that 61 cells (72.6%) showed CPs larger than 0.5 indicating a stronger activity in 'Short' than in 'Long' choice trials, whereas 23 cells (27%) showed CPs less than 0.5 indicating a weaker activity in 'Short' than in 'Long' choice trials. Recalculating CPs ignoring the direction of activity difference resulted in mean CP of 0.55. These results indicate that the spike activity during the choice-related activity component period is correlated with upcoming choice

on a trial-to-trial basis. We note that there was a considerable difference between two monkeys. The mean CPs for each animal (ignoring the direction of activity difference) was 0.56 and 0.51 for monkeys DC and NB, respectively, and all the significant CPs except one (CP=0.59) were from monkey DC. The performance of monkey DC was better than that of monkey NB (Figure 7) who never reached the performance of monkey DC even with a considerably longer training period. More works will be needed to determine whether the differential CP reflects changes in cell properties with training or other causes such as different types of cells were sampled. The example cell shown in Figure 12 was from monkey DC, and its CP was 0.645, and that of Figure 8 from monkey NB was 0.514.

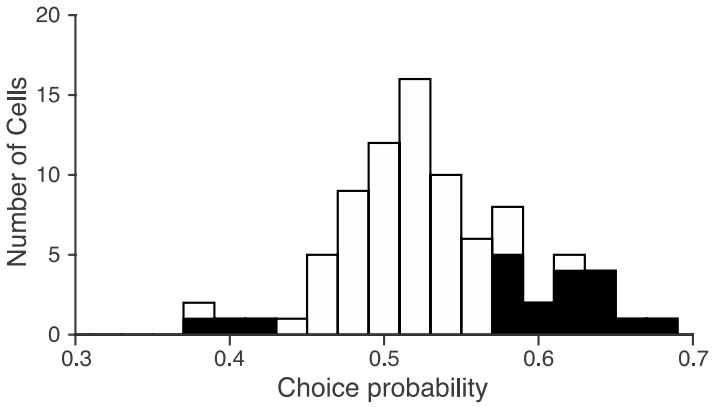

Figure 17. Choice probability in the late period. Distribution of choice probability of spike activity during the choice-related activity component period (250-520 ms of S2 onset) between 'Short'- and 'Long'-chosen trials of S50 condition from 84 cells of two monkeys. Black bars indicate statistically significant probability ($p<0.05$) as determined with a bootstrap test.

3.6. Grand mean of population spike activity

In order to see the overall trend of the activity, the normalized activity for each cell was obtained and the overall average response of all cells was obtained for each condition. In the early sensory period, activity by S1-S2 sequence conditions showed the lowest level in S30 as a whole as it can be expected by the description of pattern of interval-related activity component in 3.5.3. In the late period, there was a significant difference by choice-related activity component.

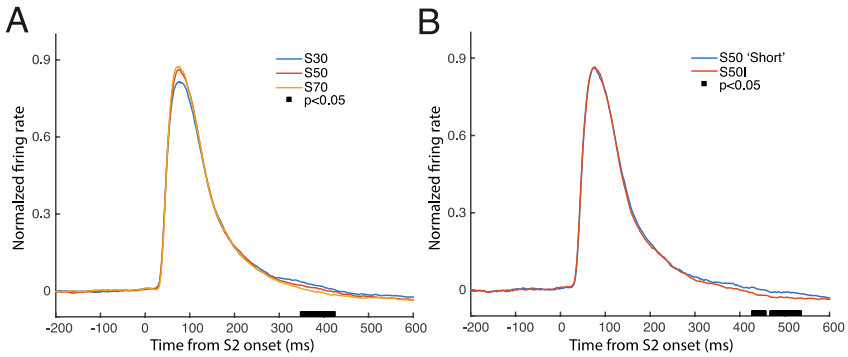

Figure 18. Standardized grand mean of activity from all cells. (A) Spike density of S1-S2 sequence conditions was normalized by the activity of S2 alone condition, and all normalized cells' activities are averaged. In grand mean, firing rate of S30 in visual response was suppressed the most. (B) Spike density of S50 trials was divided into the trials of 'Short' and 'Long' choice. The relation between the magnitude of activity and duration of SOA is not constant for all cells, making the difference in grand mean rather small in both A and B. In the late period, both interval (A) and choice-related activity components (B) were significant.

3.7. Interval-related activity component and discrimination

We next examined whether interval-related activity component is actually related to animals' discrimination behavior. For this, we took three measures as below.

3.7.1 Error trial's interval-related activity component

The activity patterns of the animals with the incorrect selection in S30 and S70 conditions were investigated. Interestingly, we observed that the activity of the error trials in a number of cells deviated from that of the correct trials. In many cases, we observed that the activity of the error trial deviated in the direction of the as a whole average of S30, S50, and S70.

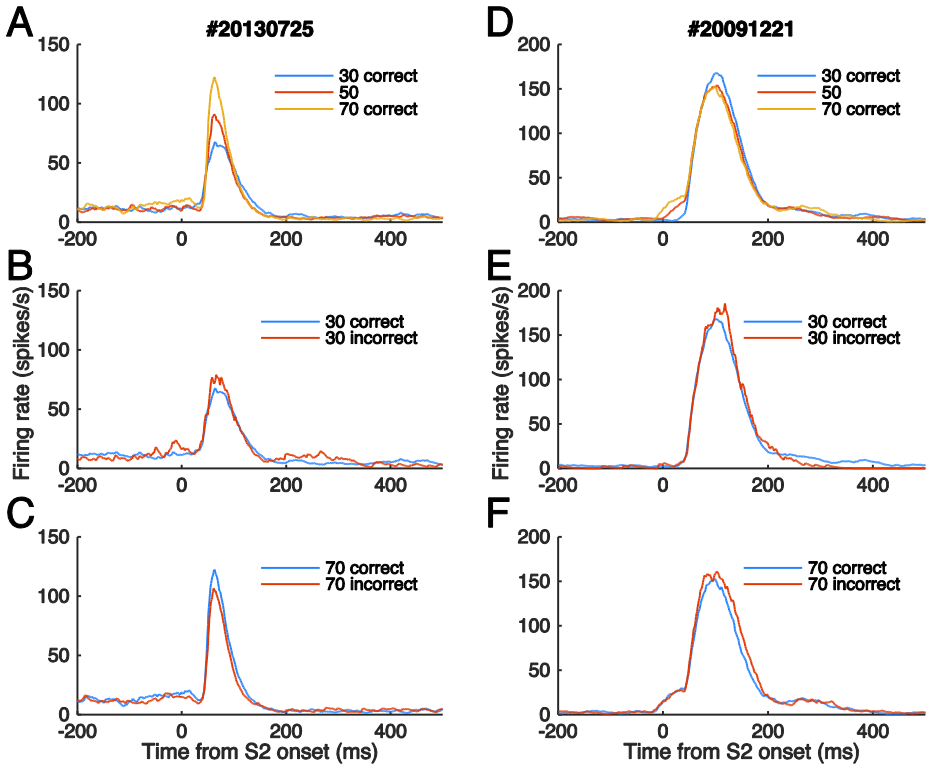

Figure 19. Comparison of activity during correct and error trials. (A-C) Spike densities of the example cell in Figure 8. (A) Mean spike density traces of the cell's activity during S1-S2 sequence conditions with correct trials only. (B) Mean spike density of S30-correct (saccade made toward the 'Short' target) and S30-incorrect (saccade made toward the 'Long' target) trials. (C) Mean spike density of S70-correct (saccade made toward the 'Long' target) and S70-incorrect (saccade made toward the 'Short' target) trials. Note that the spike density of incorrect trials in both S30 and S70 differed from the correct trials and deviated in the direction toward the grand mean. (D-F) Another example cell (#20091221). This cell was excluded as invalid because S1 evoked the criterion activity by invading the RF, but is shown here for illustration purpose. Same convention as A-C. The spike density in visual response of S70 was suppressed the most in this cell (D), and again in this cell, the activity during incorrect trials differed from that during correct trials. The spike density of incorrect trials in S70 was deviated toward grand mean (F) but, the spike density of incorrect trials in S30 was much greater than any other conditions.

3.7.2. Distance index in error trials

To further examine error trials, we divide the population DI(t) (the difference in spike density among stimulus conditions; shown in Figure 10) into correct and incorrect trials (Figure 20). Overall, the error trials did not produce a difference in distance among different SOA conditions, whereas DI of correct trials was larger than that for error trials, and thus, contributed to the overall DI in Figure 10. Note that the larger DI during the choice period is related to correct choice, and that the absence or negative DI is related to choice error – an impressive dissociation given the fact that the saccadic targets were presented 600-800 ms after S2 onset. Also note the tendency that DI is larger for correct than for error trials during the early phase, suggesting that the interval-related activity component during the early sensory period is related to the animal's choice behavior.

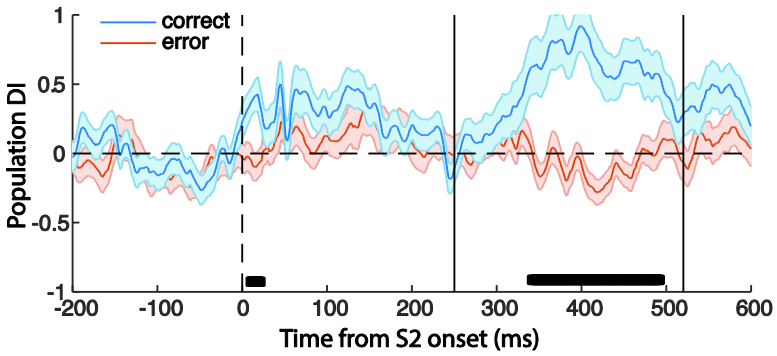

Figure 20. Population DI(t) for correct and error trials. Illustrated are the distance measures among SOA 30, 50 and 70 ms conditions calculated separately for correct and error trials; the trace in Figure10 was divided into correct and error trials. Two vertical

lines indicate the choice-related period (250-520 ms from S2 onset). Black bar under traces indicates significantly different period between correct DI(t) and error DI(t). (t-test, $p<0.05$ corrected for multiple comparison)

3.7.3 Linear discriminant analysis (LDA): predicting animal's behavior with spike activity

Linear discriminant analysis (LDA) was performed as an indirect way to investigate whether interval-related activity component could be used for animal's interval discrimination. In LDA analysis, the dissimilarity between spike trains was quantified by spike distance metric (SDM) (Van Rossum, 2001).

An exponentially-decaying kernel with short time constant was convoluted with spike trains to make spike density. In SDM, more precise spike timing could add information to help discrimination analysis and a kernel's time constant of 4ms was found to be optimal that is same with previous study's result (Van Rossum, 2001). Figure 21 illustrates that decoding accuracy increased with increasing number of cells and when using 64 cells, it exceeded criterion of 75% success rate.

LDA was performed as follows.

1) Select randomly one trial of spike density from pool of S30 and S70 trials
2) If the randomly selected spike train came from S30, average the

remaining trials except for the selected spike density to make the template of S30 and the average of the whole trials of S70 become the template of S70 and vice versa.

3) Determine how close selected spike density to the S30 and S70 templates
4) if it is close to the same SOA template, it is recorded as correct and if not, is recorded as incorrect.
5) Put the selected spike density back to the pool and repeat the above procedure (in this analysis, repeated 1000 times).
6) When increasing the number of cells, cells were also randomly selected from the entire pool of cells and the spike train was randomly chosen from the selected cells.

In sum, above three results suggests that interval-related activity component of neuronal population in V1 might help animals' actual discrimination of intervals.

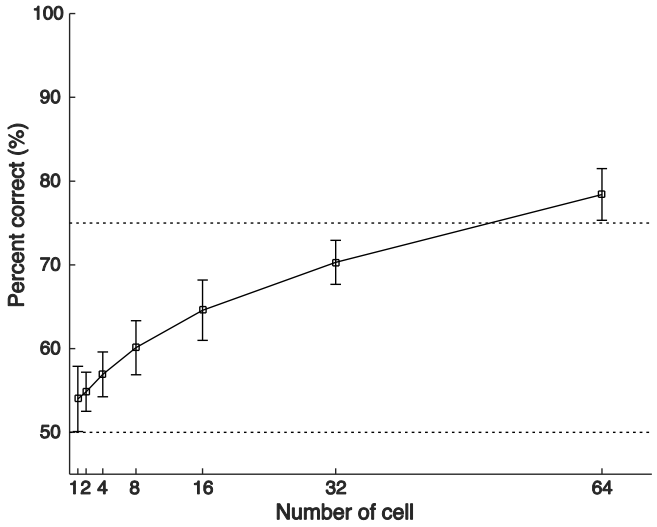

Figure 21. Linear Discriminant Analysis. Chance level of 50 % and criterion of 75 % correct rate were plotted in horizontal dotted lines. Error bars are one SE. With 64 cells, the correct rate of discrimination was larger than 75 %.

3.8. Noise correlation

Estimation of trial-to-trial covariation between spike activity and behavioral choice based on CP is limited in the presence of correlated variability of spike activity, known as noise correlation (Shadlen et al., 1996; Nienborg et al., 2012; Haefner et al., 2013). To evaluate this limitation, we calculated the Pearson's correlation coefficient for a pair of neurons that were recorded from the same electrode. The correlation coefficient during the choice-related activity component period calculated for each of 26 pairs (22 from monkey DC, 4 from monkey NB) for S50 trials ranged from -0.05 to 0.64 with the mean coefficient of 0.23. For 14 of 26 pairs, the correlation coefficient was

significant ($p<0.01$), suggesting that neural population, rather than individual cells, is probably linked to behavioral decision (Nienborg et al., 2012).

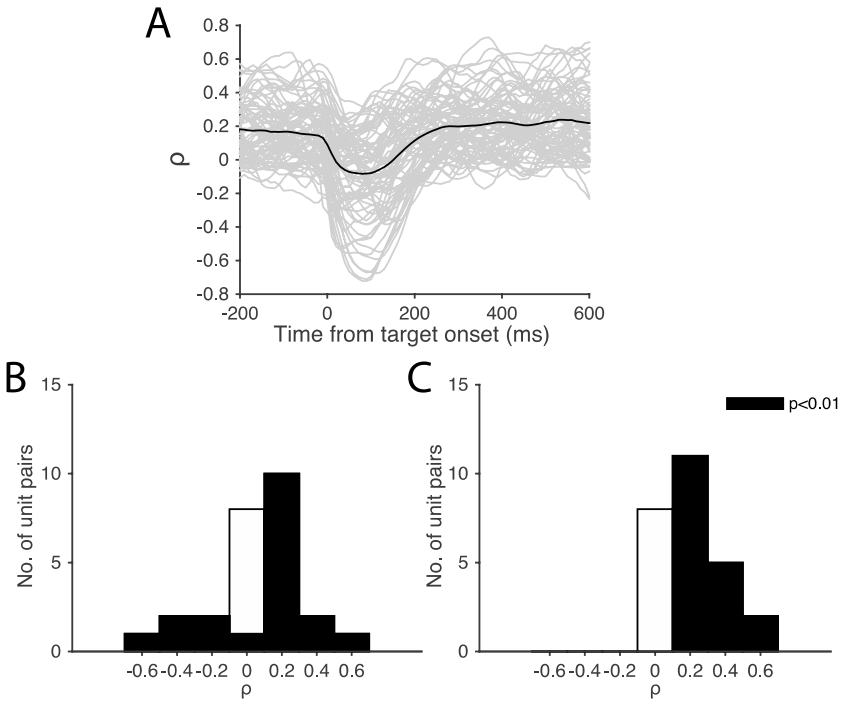

Figure 22. Noise correlation. (A) Gray traces are noise correlation time courses for each of 26 cell pairs that were recorded simultaneously from the same electrode. Black trace is the time course of average noise correlation. (B,C) Histograms of the noise correlation coefficient in early sensory (C) and the late (D) periods.

3.9. LFP response

3.9.1 LFP response of an example site

Figure 23 shows an example of the LFP response for an individual session.

In the case of S1 alone, the potential waveform that was conducted by and from the stimulus presented outside the receptive field can be seen. Typically, a large positive peak was observed first and followed by a negative overshoot by S1 alone stimulation. In the case of S2 alone, there was a typical negative deflection with two peaks. In Figure 23 bottom panel, the LFPs according to three SOA conditions were shown. The sequential arrangement of positive peaks by S1 in timed manner is conspicuous. The SOA-dependent LFP waveform was almost the same as the time-shifted linear summation of S1 alone and S2 alone waveforms in all three conditions.

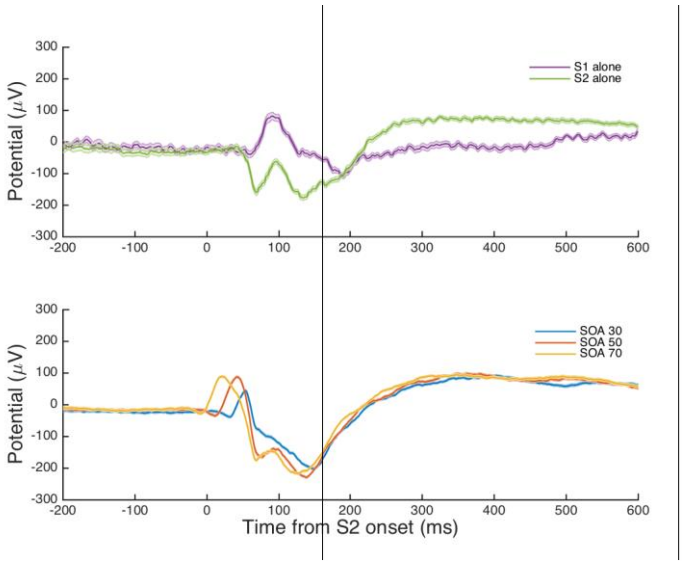

Figure 23. LFP response from an example site. (A) Mean LFP traces of S1 and S2 alone conditions. (B) Mean LFP traces of the cell's activity during S1-S2 sequence conditions.

3.9.2. Population LFP and spike activity

Averaged interval-related activity component of the LFP of all cells (Figure 24A,B) and corresponding spike activity in a normalized form were shown (Figure 24C,D). Overall, suppression was dominant during the discrimination task (Figure 24D). Specifically, during the early period suppression was the largest in S30 condition. In contrast, during the late period, the suppression was the largest in S70 condition, the smallest in S30 condition, and in-between in S50 condition.

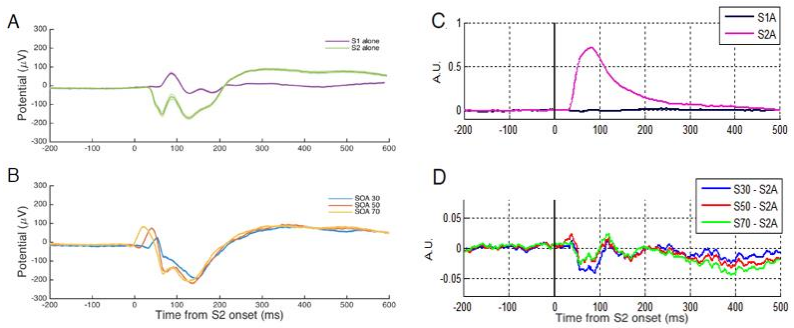

Figure 24. Population LFP and spike activity. (A,B) Shown are population LFP response. (C) Normalized population spike activity in S1 alone and S2 alone conditions. (D) Normalized spike activity in S1-S2 sequence condition minus that in S2 alone condition, revealing probably the pattern of the modulation by S1.

3.9.3. Choice-related LFP response

To see the signal associated with the choice in LFP, just like the spike

activity analysis, we examined the activity differential of S30 and S70 conditions and that of S50 'Short' and S50 'Long'. The differential trace between S30 and S70 shows a large potential change even before S2 onset. This is because S1 stimulus in S70 condition was turned on -70 ms of S2 onset. In the late period, similar negative deflections can be seen in both differential traces, revealing the choice-related LFP activity component.

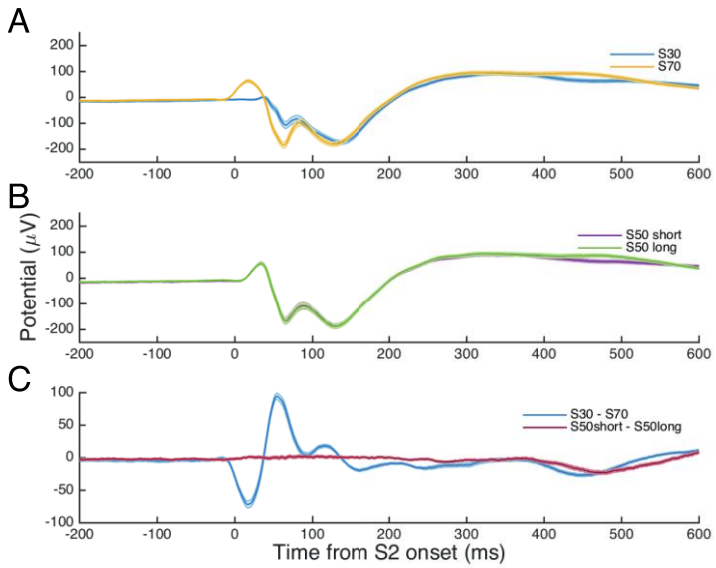

Figure 25. Choice-related LFP activity component. (A) Shown are the mean LFP traces of S30 and S70 conditions. (B) Shown are the mean LFP traces of S50 'Short' and S50 'Long' conditions. (C) Differential trace between S30 and S70 conditions and that between S50 'Short' and S50 'Long'.

3.9.4. Choice-related LFP spectrogram

Figure 26A shows the LFP spectrogram difference between the mean S30 and mean S70 conditions. For this, spectrogram was computed for each trial of the same SOA condition, averaged over all trials and then across all cells, and then subtracted (Figure 26B). The LFP spectrogram difference between the mean S50 'Short' and mean S50 'Long' conditions were computed in the same way (Figure 26B).

The strong difference of power density due to the different SOA (S30 and S70) was shown in frequency range corresponding to 30 - 70 ms (14 ~33 Hz) - 70 to around 200 ms of S2 onset while the similar negative power density in the low frequency range (dominantly below 15 Hz) after about 300 ms of S2 onset is visible in both Figure 26 A and B, suggesting the choice-related activity component.

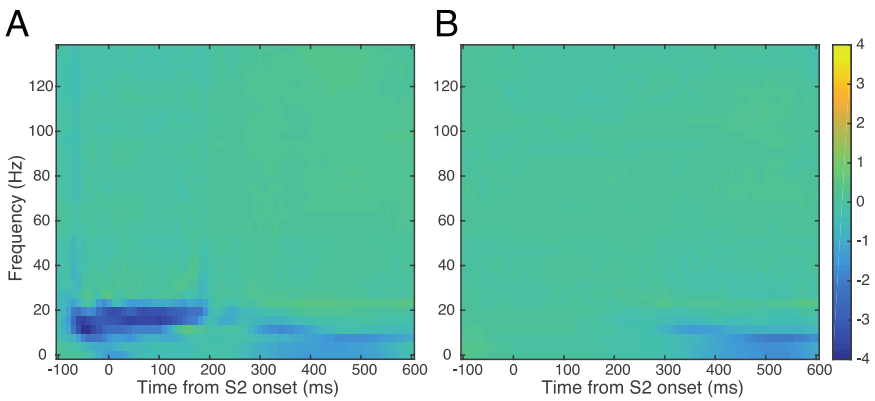

Figure 26. LFP spectrogram of the choice-related activity component. (A) Interval-related LFP spectrogram. (B) Shown similarly is the LFP spectrogram difference between the mean S50 'Short' and mean S50 'Long' conditions. Color bar indicates power density difference in dB.

,

3.10. Reward-related activity component

After an animal's choice made to the saccade target, once its decision was correct, solenoid valve that was attached between juice reservoir and hose opened and closed three to five times and small number of drops of juice were delivered to a monkey. This period of reward given, we examined the signals related to reward in LFP and spike density.

We examined reward-related activities in V1 in three different periods.

1) Reward period (period after saccade onset)

2) Fixation period (period between fixation onset and stimulus onset, in next trial)

3) Visual response (period after S2 onset)

3.10.1. Reward period

3.10.1.1. Saccade onset aligned LFP

In order to investigate reward effects, we first checked saccade onset aligned mean LFP waveforms of each rewarded and unrewarded trial. Figure 27 shows sessions with and without reward-related effects for each animal. In this figure, all trials, regardless of SOA conditions and animal’s choice, are averaged, sorted only by reward. In most sessions, both animals showed

different LFP amplitudes under rewarded and unrewarded conditions, typically in the 300-550 ms duration from the saccade onset. Note that actual juice reward given duration is indicated in figure 35 (see 3.10.1.5.). The same pattern was shown when the SOA and choice was controlled. There were sessions in both animals that showed no difference in LFP waveform between rewarded and unrewarded in less than 10 % of whole sessions. Thus, the reward-related LFP activity component is variably visible across sites, and when it is, the period was similar. Note that the time course of LFP traces were similar between rewarded and unrewarded trials within each animal, and the trace went negative in association with the reward event.

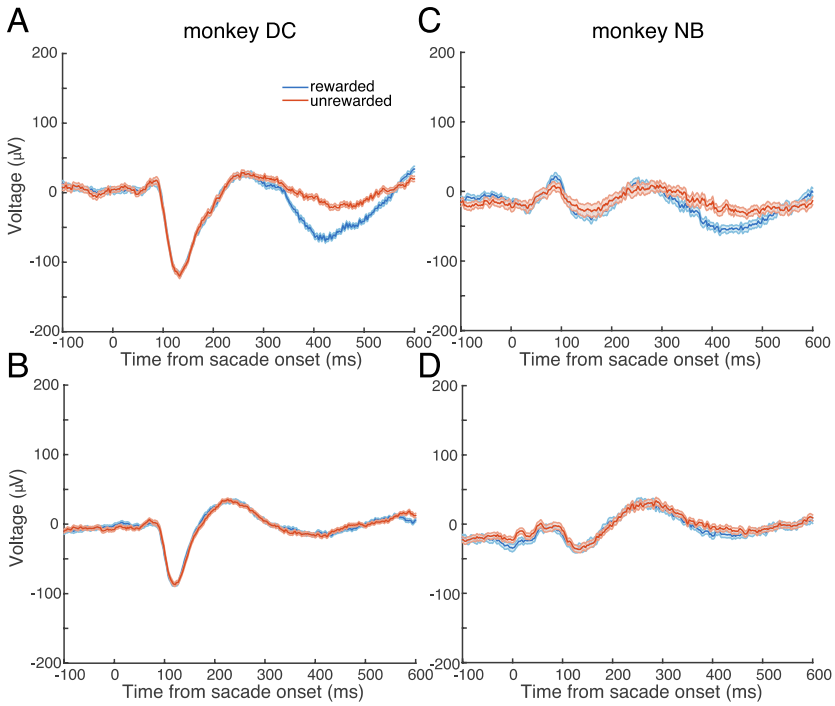

Figure 27. Reward related LFP activity component in example sessions from monkey

DC (A,B) and monkey NB (C,D). (A) Mean LFP traces in rewarded and unrewarded trials in a representative session. The difference between these two traces after about 300-550 ms of saccade onset suggests a reward related activity component. (B) Data from another example site, but with no apparent reward related activity component. (C) Data from a session in monkey NB in which a rewarded related LFP activity component is apparent during the period similar to that of A. (D) Data from a session with no reward related activity component.

Population response also showed a clear difference in LFP amplitude according to the reward. To validate the significance of the reward-related activity component, we took steps to determine reward-related signal and validated the rejection of the possible confounding source, next.

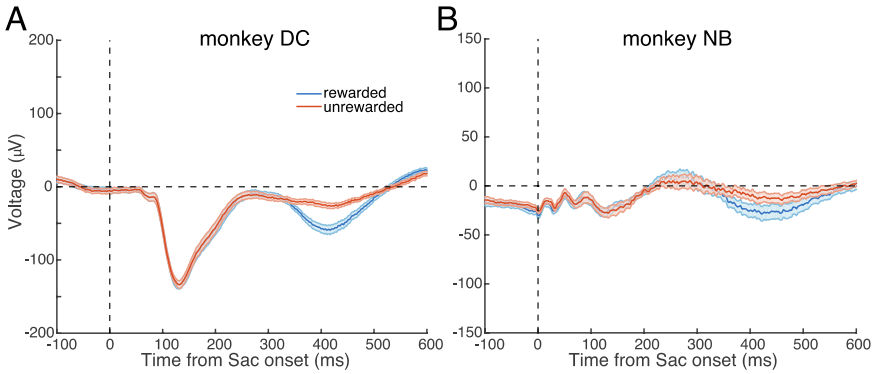

Figure 28. Reward related population LFP activity component. Similar to Figure 27, but averaged over all sites within monkey DC (A) and monkey NB (B).

3.10.1.2. LFP response by saccadic directions

In order to clarify the Reward effect, we investigated whether there would

be a conflicting condition. We checked whether there was a difference in waveform of LFP under all conditions.

Figure 29 illustrates LFP waveforms according to all available conditions, ie., combination of choices (‘Short’ and ‘Long’) and arrangements of saccade target presentation a / b. Each average waveform of LFP was different according to each condition. We observed that LFP deviated much in the ‘Long’ b condition compared to other three conditions in both animals. This turned out to be the visual reafference when animal made left saccade cell's RF or RF surround affected by residing the alternative ‘Short’ target in lower-left (this was only possible in choice ‘Long’ and b condition). Even spike activity was evoked for NB in ‘Long’ b condition (figure 30B).

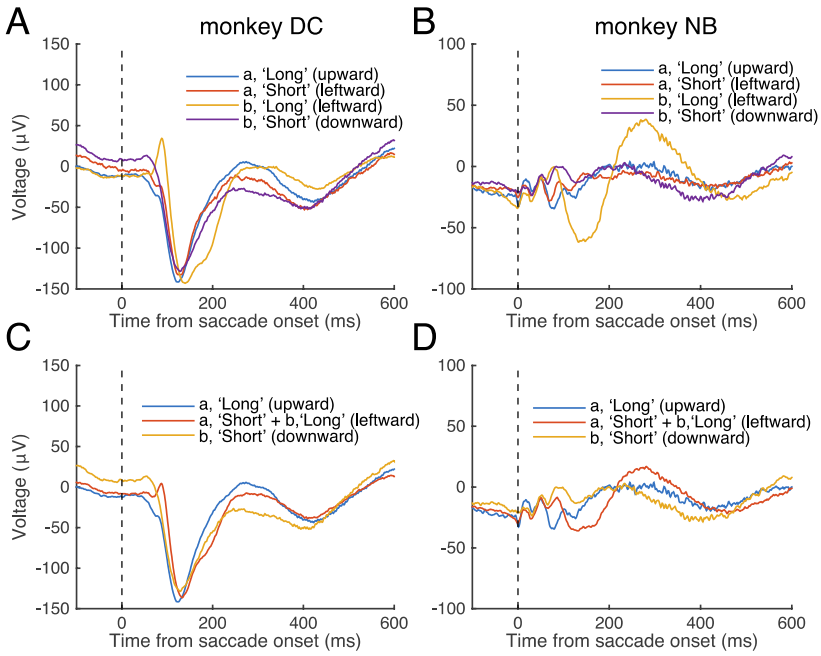

Figure 29. LFP waveform dependence on saccade direction for monkey DC (A,C) and

monkey NB (B,D). (A,B) LFPs for four conditions (combination of saccade target condition a/b and choice 'Long'/'Short'). (C,D) LFPs sorted by saccade directions. Note the potential difference in waveform according to four conditions. Thus, we first computed reward related activity component separately for each of four conditions and then pooled them. A large voltage change in the 'Long' choice during the saccade target condition b, especially monkey NB (B) that is distinguished from the rest of conditions is due to the visual reafference signal caused by the saccade target representing 'Short' that sweeps into the cell's RF during the choice saccade toward 'Long' (see text).

The difference of LFP response among conditions seems to be a different saccade direction. The LFP waveforms is considered to show a sequential change according to the direction of the saccade in the upper-left, left, and lower-left directions.

Therefore, we controlled Long/Short and a/b conditions for reward-related activity component in further analysis. After we calculated differences between rewarded and unrewarded trials in each condition, we pooled the activities and derived reward-related signal.

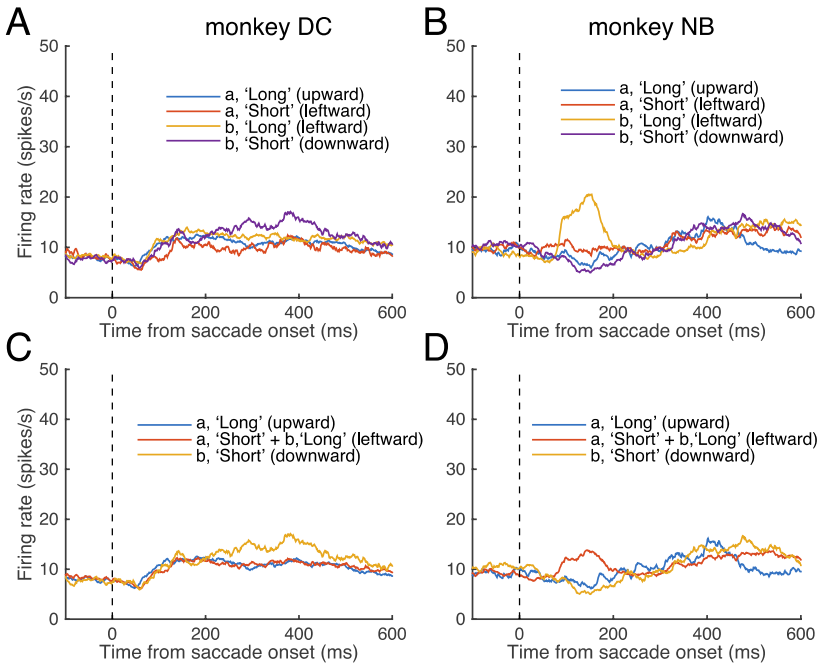

Figure 30. Spike density dependence on four conditions. Convention is the same as Figure 29 except neural activity is the spike density. As in Figure 29, a distinct spike activity in the 'Long' choice during the saccade target condition b in monkey NB (B) reflects the visual reafference signal.

3.10.1.3. Extraction of reward-related activity component

In order to remove the LFP dependence according to the saccadic direction, we obtained the rewarded minus unrewarded activity for each condition and then combined the four into one for each session (Figure 31). In the four LFP waveforms, only reward effect remain after dependency on saccadic direction was subtracted out and LFP waveforms show very similar trace. Note that the LFP trace of 'Long' b condition is also not deviated from that of other three

conditions so that it suggests that artifact by visual reafference was removed in both monkeys (Figure 31 A,B). Resulted reward-related LFP activity combined from the split four show very clear negative deflection in the similar period in both monkeys (Figure C,D).

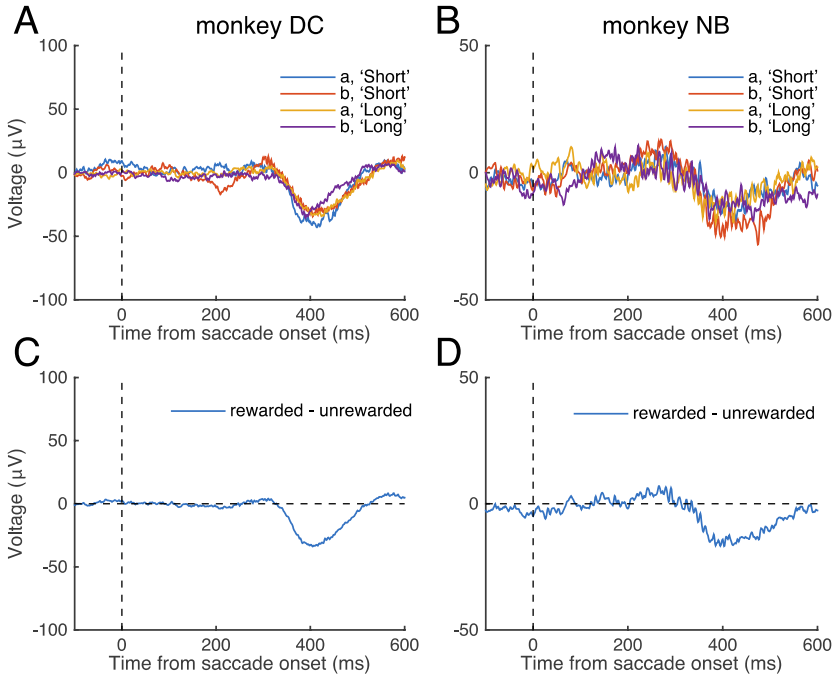

Figure 31. Calculation of reward related signal for individual session. (A,B) Mean unrewarded LFP was subtracted from the mean rewarded LFP separately for each of four conditions in both monkeys. (C,D) Average of four conditions in A and B.

3.10.1.4. Subthreshold LFP of reward-related activity component

As in the individual session results, significant reward-related activity component from all sessions occurred in very similar period in both animals; 346-497 ms of saccade onset for DC, and 356-513 ms of saccade onset for NB.

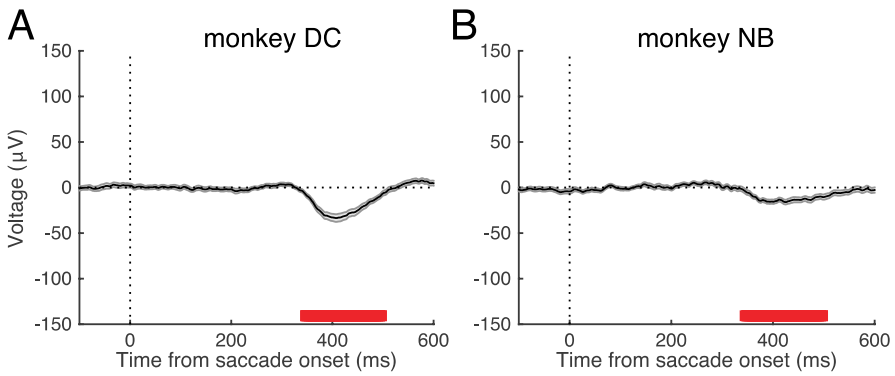

Figure 32. Reward related population activity component. (A) Average of reward related activity component from all sessions in monkey DC. Significant deviation from zero (red bar on the x-axis) appeared during the period of 346–497 ms after saccade onset (t test, $p<0.05$). Shade indicates 1 SE. (B) Average of reward related activity component from all sessions in monkey NB. Significant period was 356–513 ms after saccade onset (t test, $p<0.05$), comparable to monkey DC.

However, the difference according to reward was not visible in spike activity in both monkeys. This suggests that the reward-related LFP activity component is subthreshold to spike initiation. (Figure 33 C,D)

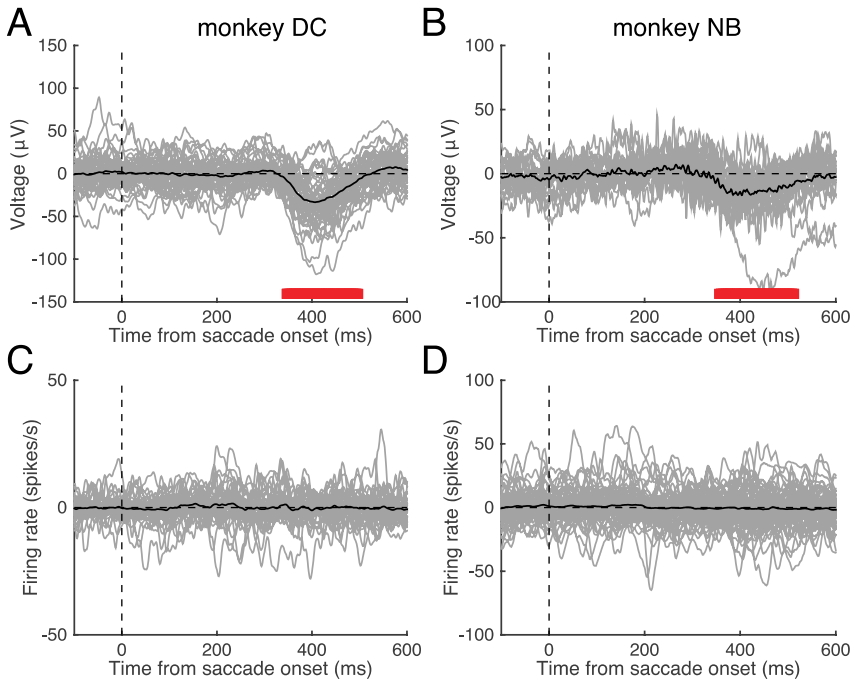

Figure 33. Rewarded LFP (A,B) and spike (C,D) activity. (A) Average of reward related activity component from all sessions in monkey DC (black trace) with traces from individual sessions (gray traces) overlaid. (B) Monkey NB with the same LFP traces as A. (C) Spike density difference between rewarded and unrewarded computed in the same way as LFP in monkey DC. (D) The same as C with monkey NB. Note that unlike LFP, there is no significant difference in spike activity, suggesting that the reward related LFP activity component is subthreshold to spike initiation.

When we examined spectral power density difference between rewarded and unrewarded cases, the difference in power density was seen in the same duration seen in above LFP waveforms, dominantly in the lower frequency band. (under 15 Hz)

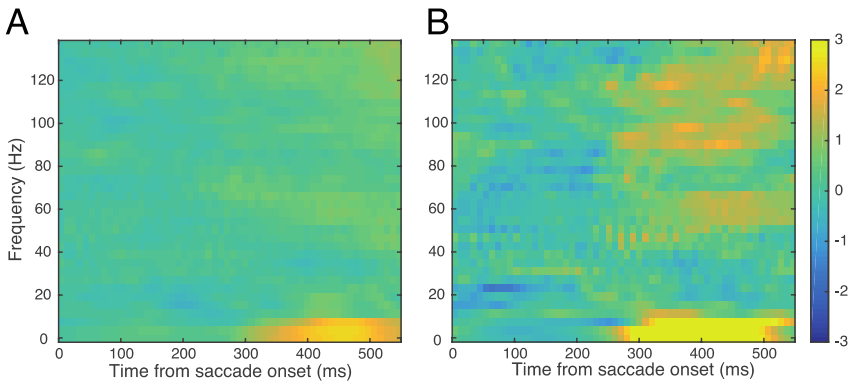

Figure 34. LFP spectrogram of the reward related activity component. Mean rewarded spectrogram minus the mean unrewarded one across all sessions (A), and for one representative session (B). Color bar indicates power density difference in dB.

3.10.1.5. Control of solenoid valve sound

When reward was given to an animal, solenoid valve always sounded simultaneously so it could be a confounding source for reward-related activity component. Therefore, we collected the additional valve sound controlled data from four sessions in monkey NB. Among general blocks, we put small number of different blocks which were to collect valve sound-controlled data with exceptional care. In those blocks, we removed juice from the reservoir so that when rewarded times no actual juice was given to an animal but still solenoid valve sound existed. This could disencourage an animal and even be able to spoil a monkey's learned behavioral performance so the number of collected trials had to be limited. Two out of four sessions were discarded because collected number of trials from control blocks in those sessions turned out to be not enough to analyze for this purpose. The one session showed reward-related

activity component from trials in general blocks while the remaining one session showed none. (Note that majority of sessions showed reward-related LFP signal but small number of sessions didn't show this.)

As shown in monkey NB population data (Figure 33B), reward-related difference of trials from general blocks is visible in the similar period while that of trials from control blocks is not (Figure 35B). During the period 356-513 ms of saccade onset, valve sound did not evoke field potential difference and this suggests that actual delivery of reward is related to the reward related LFP activity component, and that the solenoid valve sound itself might not be the source of it.

Actual juice reward given duration is indicated with black under the traces in Figure 35 B.) and overall time difference between saccade onset and reward onset time of all sessions was 270.5 (±22.2) ms.

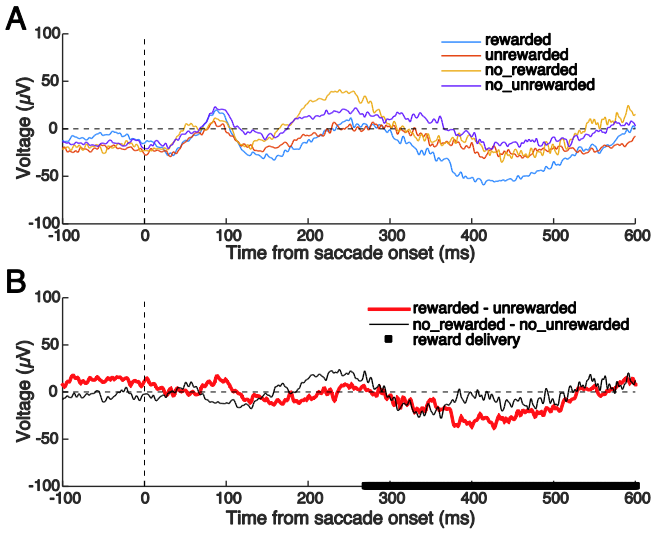

Figure 35. A control session for the sound associated with solenoid valve operation. (A) Rewarded and unrewarded LFP traces from general blocks are shown with those traces from special blocks in which the solenoid valve operated but no reward was delivered. No-rewarded trace indicates LFP response when juice was not delivered to the animal even if valve operated in the control blocks just like the general blocks. No-unrewarded trace was unrewarded cases from the control blocks. A small number of control blocks were inserted among general blocks. (B) Reward related LFP activity component appeared during the trials from the general blocks, but it did not during the trials from the control blocks. These suggest that actual delivery of reward is related to the reward related LFP activity component, and that the solenoid valve sound itself might not be the source of it. Black bar in x-axis indicates the time of valve operation.

Below is another one session where solenoid control blocks were acquired. When the reward related LFP activity component in the general blocks is not observable for a given site, no activity difference is observed between rewarded and unrewarded trials in the control blocks, and this suggests that the sound associated with the solenoid valve operation did not cause the LFP activity changes.

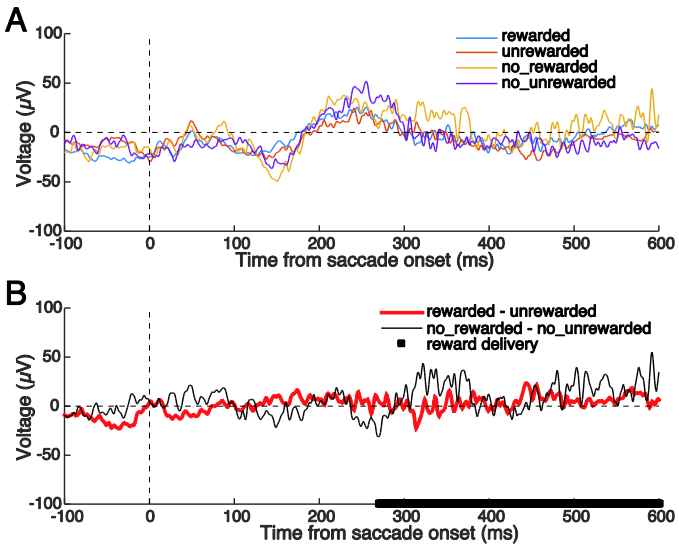

Figure 36. Another control session for the sound associated with solenoid valve operation. (A) Mean LFP activity for rewarded and unrewarded trials from the general blocks and for no-rewarded and no-unrewarded trials from special blocks. (B) The results suggest that when the reward related LFP activity component is not observable for a given site, no activity difference is observed between rewarded and unrewarded trials in the control blocks, and that the sound associated with the solenoid valve operation did not cause the LFP activity in association with reward event.

3.10.2 Potential effects of reward on next trial (1): Modulation of spontaneous activity level

3.10.2.1 LFP response in fixation period

The LFP response associated with previous trial's reward event in the fixation period was investigated. For monkey DC, there was significant difference in LFP in duration of 335 - 434 ms after fixation onset among four

conditions (F-test, $p<0.05$). Note that in significantly different duration, two rewarded traces grouped to be more positive than the two unrewarded traces. When we examined the LFP again sorting by reward history of preceding trials, we were able to confirm statistically significant difference in the period 335 - 437 ms of fixation onset (t-test, $p<0.05$). This difference was greater in animal DC. For respective LFP traces for monkey NB, the LFP tended to be more positive when the preceding trial was rewarded like DC. Every session showed variable difference that resulted in small LFP activity difference associated with previous reward, therefore, in monkey NB, this difference was nonsignificant unlike monkey DC.

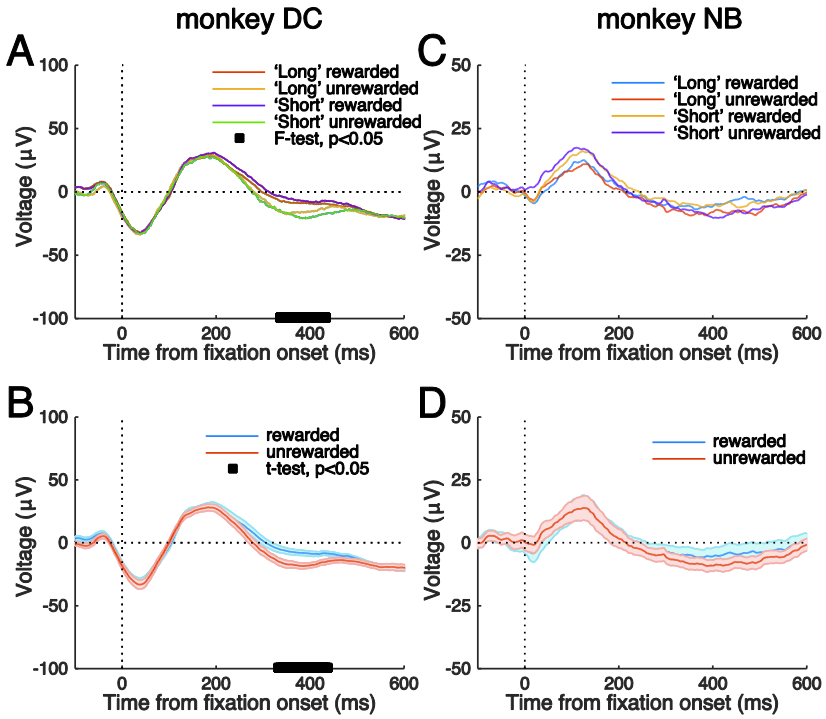

Figure 37. Effects of reward on the LFP activity of next trial. (A,C) Population LFP traces divided into four groups according to the combination of choice and reward history of immediately preceding trials for each monkey. (B,D) Population LFP traces sorted by reward of immediately preceding trials but combined regardless of choice. The traces from monkey DC were significantly different in the period of 335-434 ms of fixation onset (F-test, $p<0.05$, corrected for multiple comparison) and 333-437 ms (t test, $p<0.05$, corrected for multiple comparison) in A,B. (C,D) Respective LFP traces for monkey NB. The LFP tended to be more positive when the preceding trial was rewarded like, but unlike monkey DC this difference was nonsignificant.

In difference LFP spectrogram between the spectrogram for which the preceding trial was rewarded and that unrewarded (Figure 38), spectral power density difference was not vivid unlike in the reward period (Figure 34A). Only small negative power density difference (~ -0.4 dB) existed in low frequency

band (under 20 Hz), while small positive power density difference (~ +0.3 dB) resided in high frequency range (over 70 Hz).

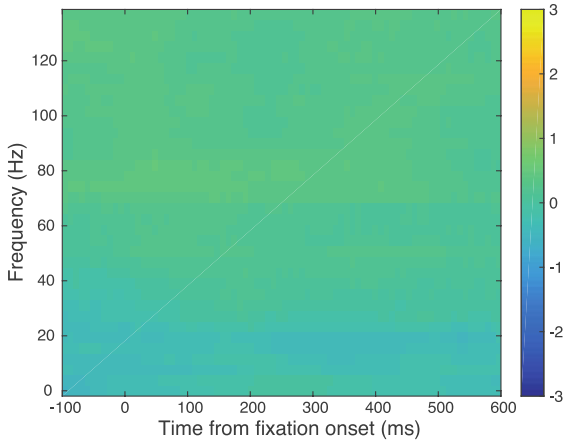

Figure 38. Difference LFP spectrogram between the spectrogram for which the preceding trial was rewarded and that unrewarded. Same convention as Figure 34A. Unlike Figure 34A, no distinctive spectral power difference by reward history was apparent.

3.10.2.2 Spontaneous spike response in fixation period

Figure 39 illustrates that the possibility of potentially different level of spontaneous spike level during fixation period depending on whether the previous trial was reward or not

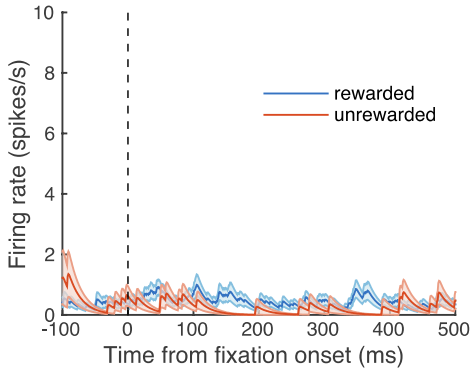

Figure 39 Spike density from a representative session, illustrating the potentially different level of spontaneous spike level during fixation period depending on whether the previous trial was reward or not. Mean firing rates were significantly different (fixation period: 0-500ms of fixation onset, t-test, $p<0.05$)

First, population firing rate calculated over a period of 0-500 ms of fixation onset time show no difference between rewarded preceding trials and unrewarded preceding trials.

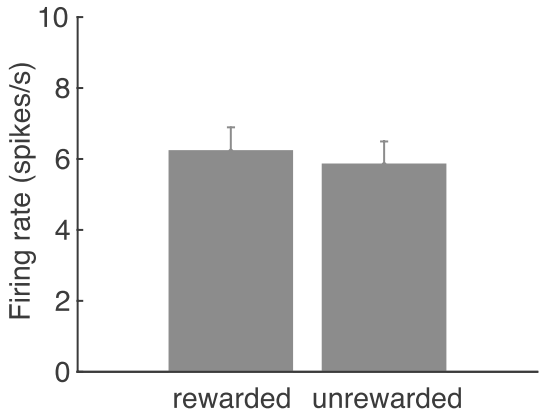

Figure 40. Effects of reward in preceding trials on the spontaneous spike activity level during fixation period. Shown are population firing rate calculated over a period of 0-500 ms of fixation onset time. The mean firing rate for rewarded preceding trials was

6.2 (±0.67) spikes/s, and that for unrewarded preceding trials was 5.84 (±0.64) spikes/s.

For individual cells, there were 13 cells statistically significant (t-test, $p < 0.05$) out of 84 cells in mean firing rate difference in fixation period according to previous trial's reward event. Twelve cells out of above 13 cells were from monkey DC and one from monkey NB. Overall 84 cell's mean firing rate difference was 0.38 spikes/s and it was significantly different in population (Wilcoxon signed-rank test, p = 1.58e-04). However, there was a difference between monkeys in this analysis. Population mean firing rate difference was dominantly due to monkey DC whereas little preceding trial's reward related effect was found in monkey NB with one significantly different cell in mean firing rate difference in fixation period.

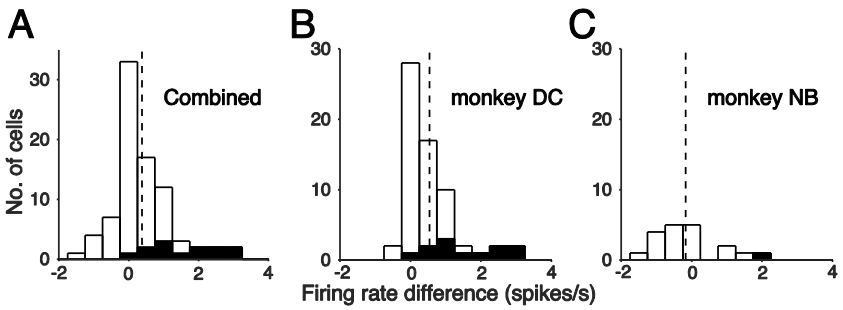

Figure 41. Histogram of the difference in spontaneous spike activity level between the rewarded and unrewarded preceding trials for combined (A), monkey DC (B), and monkey NB (C). Black filled bar indicates the cells with a significant difference in spike activity; 13 cells (15%) showed a significant difference out of 84 cells. The mean firing rate difference (vertical dashed line) was 0.38 spikes/s and this was significantly different from zero (Wilcoxon signed-rank test, p = 1.58e-04) in A. This difference was mostly due to monkey DC, and the mean difference was 0.54 spikes/s (p = 1.94e-08) in

monkey DC. In monkey NB the mean difference was -0.17 spikes/s and was insignificant ($p = 0.18$).

The mean firing rate difference according to preceding trial's reward event in fixation period was not due to differential occurrence of microsaccades. The mean numbers of microsaccades counted during the fixation period (0-500 ms of fixation onset) were 1.15 (±0.08) and 1.18 (±0.10) for rewarded and unrewarded cases, respectively, and there was no significantly different cells in population.

3.10.3 Potential effects of reward on next trial (2): Modulation of visual response

Three out of 84 cells were found to show modulated visual response by reward in the preceding trial (Figure 42,42,44). All three cells had two peaks in visual response and modulation was observed only near the delayed second peak. Two cells had a strong delayed activity in the unrewarded case (Figure 42,43), whereas the one cell had a strong delayed activity in the rewarded case (Figure 44). For first example cell (Figure 42), the reward related modulation was mostly from the SOA of 30 ms condition, however, unlike the cell of Figure 42, the SOA selectivity was absent in the latter two example cells.

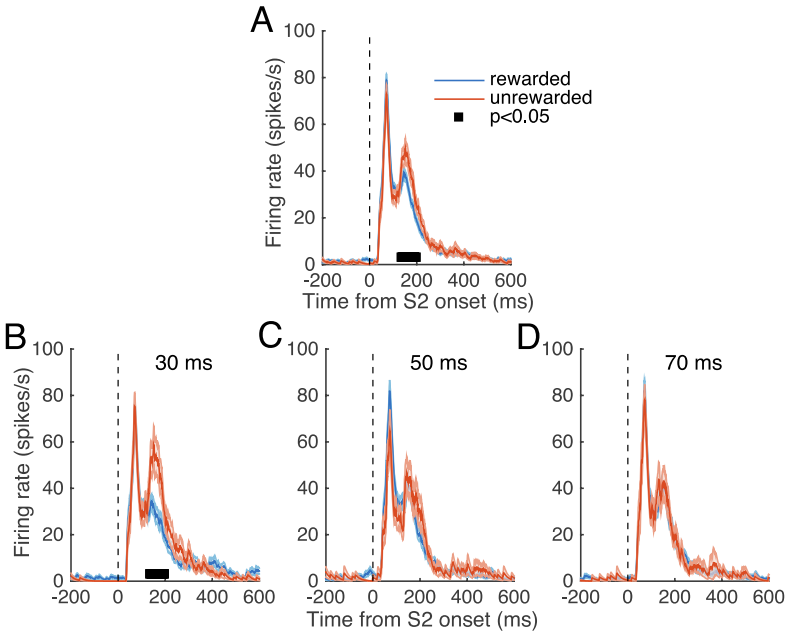

Figure 42. Modulation of visual response by reward in the preceding trial in an example neuron. (A) Overall spike activity following the onset of S2 at the RF two groups of trials divided by the reward in the preceding trial. The delayed activity was reduced when the saccadic choice was rewarded in the preceding trial compared to when unrewarded. (B-D) The trials were divided according to SOA of the current trial, 30 (B), 50 (C), and 70 ms (D). The reward related modulation was mostly from the SOA of 30 ms condition.

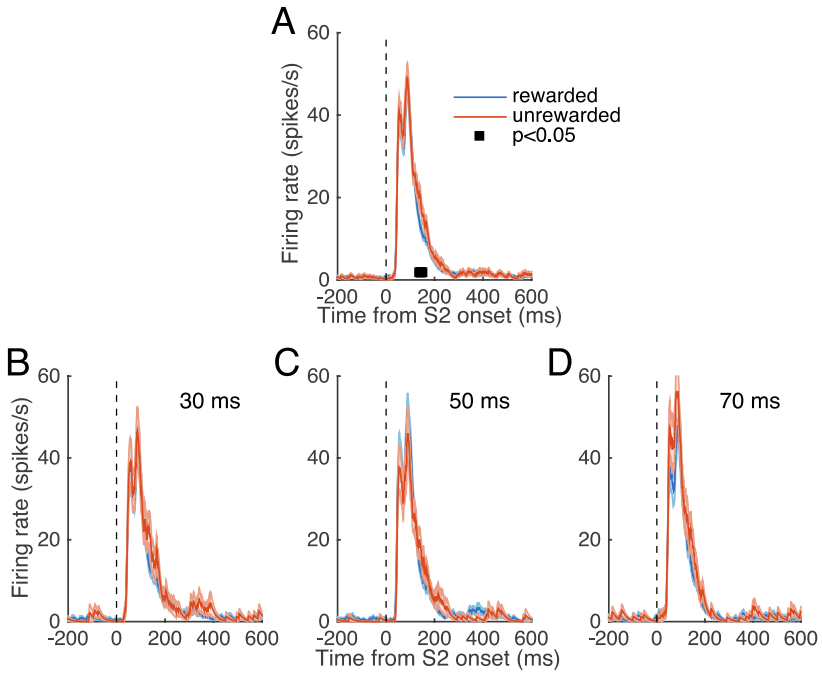

Figure 43. Modulation of visual response by reward in the preceding trial in another example neuron. Same convention as Figure 42. Like the cell of Figure 42, the delayed activity was significantly modulated depending on whether reward was delivered in the preceding trial. However, unlike the cell of Figure 42, the SOA selectivity was absent.

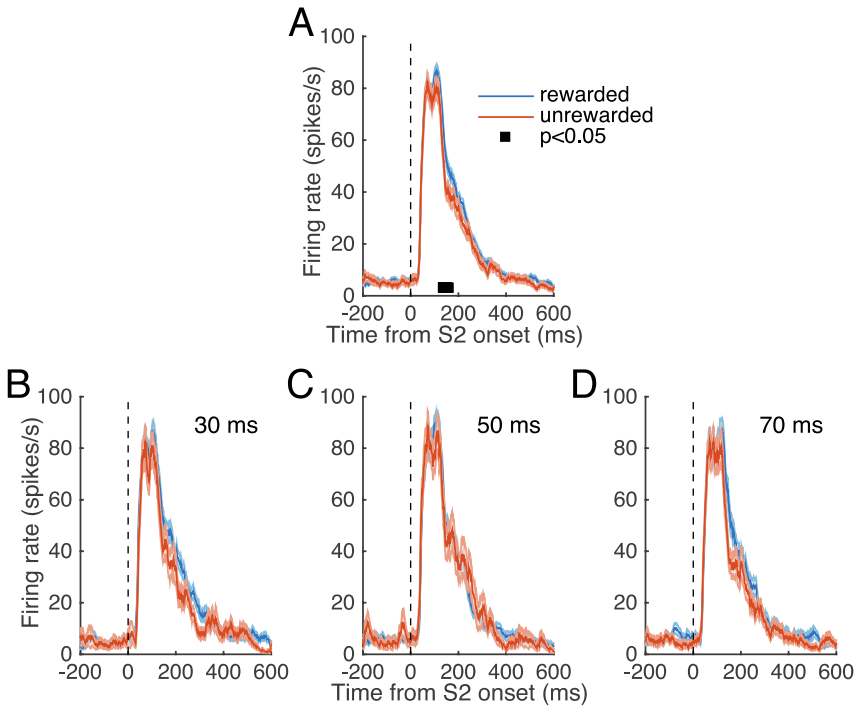

Figure 44. Modulation of visual response by reward in the preceding trial in yet another example neuron. Convention is the same as Figure 42. In contrast to the former two example cells, the activity increased when the reward was delivered in the preceding trial. However, consistent with the cells of Figures 42 and 43, the modulation of activity occurred during a delayed period, rather than during the initial visual response.

Three anecdotal cases were found in 84 cell populations. Although modulation tendencies for the preceding trial were observed in not that consistent way in the three cells, but there is a possibility that modulation on the visual response due to the reward history may exist.

3.10.4. Behavior depending on reward history

We next investigated whether reward history affects animal's behavioral choice. Well-trained animals are almost correct in their decision in S30 and S70 conditions. In S50, reward was delivered to the animal in randomly half of S50 trials regardless of their decision. We therefore examined whether the reward history for animals in the S50 condition affects the future choice of animals.

Once SOA 50 ms interval stimuli presented to monkeys and animals made their decision, there are four combination situations according to choices and reward events. We defined *'Go Long' X* variable as follows. The *'Go long' X* was set to 1 in the two conditions (rewarded for 'Long' and unrewarded for 'Short' choice), which are likely to lead the animal's long choice, and remained two conditions (rewarded for 'Short' and unrewarded for 'Long') was set to 0. For the previous 10 trial history, logistic regression was performed to analyze whether previous *'Go Long' X* variables affected current animal's decision.

'Go Long' X =

	Long choice	Short choice
reward	1	0
No reward	0	1

$$\text{Logit}(b0 + b1*Xn\text{-}1 + b2*Xn\text{-}2 + ,\ldots, b10*Xn\text{-}10) = Yn$$

(Where Xn is *'Go Long' X* of nth trial, *Yn* is animal's choice of nth trial and *bs* are beta coefficients. Monkey's choice variable Y was 1 when 'Long' chosen and 0 when 'Short' chosen.)

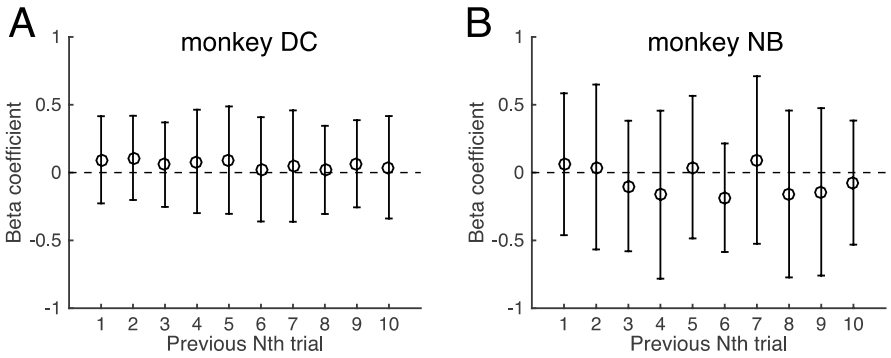

Figure 45. Beta coefficients of logistic regression analysis in monkey DC (A) and monkey NB (B).

No consistent beta was found in every session in both animals and no beta was significant in all sessions in both monkeys.

In Figure 46 illustrates animals' current trial's choice behavior depending on previous trial's Go Long X. When previous Go Long X variable was 1, that was, the reason for an animal to choose 'Long' decision was likely to be high, the probability of an animal's long selection tended to increase across three SOA conditions in the current trial in both animals.

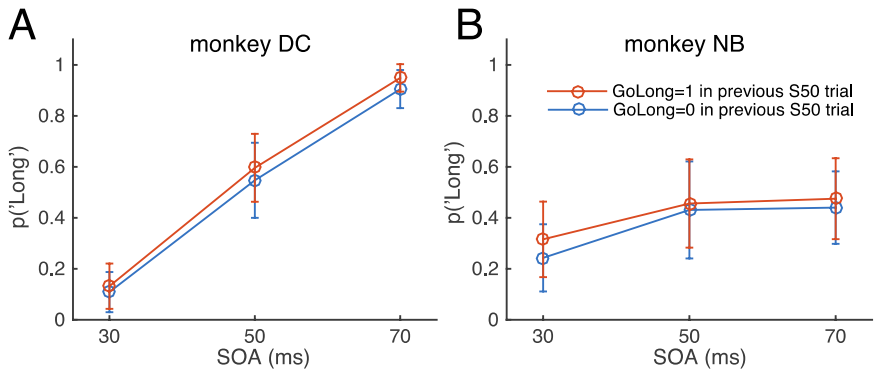

Figure 46. Probability of saccadic choice toward the 'Long' target as a function of SOA. The probability tended to increase when the 'Go Long' X variable was 1 (rewarded for 'Long' and unrewarded for 'Short' choice) in the preceding trial for both monkeys.

4. Discussion

4.1. Interval timing based on surround interaction

Major finding of the present study is that single V1 neurons show a differential activity according to the temporal interval between two events across RF boundary during initial sensory period. This interval-related activity modulation is based on interaction between RF center and surround, and sensitive to tens-of-milliseconds interval. Temporal aspects of center-surround interaction were examined previously (Bair et al. 2003; Muller et al. 2003). The mechanism of interval-related activity component is probably related to the collinear suppression or facilitation induced by S1 of subsequent feedforward inputs from S2, as hypothesized for enhancing contour extraction (Paradis et al. 2012). The effects of SOA may be related to the latency of these modulations, suggesting a role of cortical networks for computing temporal delay (Buonomano 2003; Goel and Buonomano 2014). The interval-related activity component found in the present study probably reflects relative interval (shorter or longer), since the latency of surround suppression depends on suppression strength (Bair et al. 2003). We expect our results to provide new insights into the mechanisms of how tens-of-milliseconds interval can be timed and how visual motions that extend beyond the classical receptive field (Hedges et al. 2011) can be processed in the brain.

The function relating the magnitude of neural activity and the interval

was not always monotonic; a shorter interval was associated with a lower activity for most cells, but with a higher activity for some other cells. This is contrasted with the monotonic relationship reported for timing of relatively long intervals (Mayo and Sommer 2013). The non-monotonic relation of the interval-related activity component found in the current study may be due to its mechanism. A point stimulus generates a 'point image' in the visual topographic representations (Grinvald et al. 1994; McIlwain 1975) that decays with space and time (Schwartz et al. 2007). Within the spatiotemporal window of the 'image' generated by S1, the magnitude of response to S2 will be modulated in relation to the temporal interval. However, other factors may also influence the pattern of interval-dependency. It is known that feedback inputs modulate the time course of activation in sequential presentation of stationary stimuli (Ahmed et al. 2008), and hence raising the possibility of modifying the pattern of SOA-dependency. Both suppressive and facilitative interactions occur from surround, variably modulating response magnitude. Although response suppression is the rule for surround interaction, collinear Gabor patches in the flanking zone, as used in the present study, also induce response facilitation (Mizobe et al. 2001).

Is interval-related activity component indeed related to the signal for interval discrimination, or simply activity modulation related to visual metacontrast masking? Visual masking is a perceptual phenomenon in which perception of a visual stimulus is influenced by the presence of another stimulus, called a mask. Metacontrast, as a type of visual masking, occurs when the mask does not spatially overlap with the target stimulus to be detected, and the target

stimulus is often a small dot and the mask is an annulus that surrounds the dot. It has been hypothesized that feedforward and feedback activation involving V1 are related in expression of metacontrast (Silverstein 2015). It is possible that the modulation of V1 neural responses to the RF stimulus (S2) by the surround stimulus (S1) with the SOAs used in the current study is related to a forward (the mask temporally preceding the target) metacontrast masking. While the modulation of neural activity based on the surround interaction of this kind may be a candidate neural correlate of metacontrast masking, there are also evidences that suggest otherwise; preliminary evidence suggests that the S1 presented later than the S2 with SOA of up to 100ms showed little effect on V1 spike activity (Kim et al., unpublished), suggesting that the surround interaction observed with stimulus sequences used in the current study is unlikely to underlie metacontrast masking. A study by von der Heydt et al. (1997) suggested that the activity of neurons in areas V1 and V2 in the monkey is not compatible with metacontrast masking; cells that responded to a uniform test stimulus covering the RF were not affected by the mask; no cells were suppressed at an SOA of over 50 ms, thus short to account metacontrast masking in the range of more than 200ms. They suggested that metacontrast masking occurs beyond V1 and V2. A study on V4 (Kondo and Komatsu 2000) showed a longer SOA range, but concluded that the activities of V4 neurons either do not parallel the perception in metacontrast masking; the V4 neurons tended to have a shorter duration of suppression; still shorter SOA range and symmetrical pattern of the magnitude of suppression about 0-ms SOA in V4 whereas the suppression in the perceptual metacontrast masking

studies is relatively asymmetrical (Schiller and Smith 1966).

We provided two evidences that the interval related activity component is indeed related to the signal for interval discrimination. First, the interval-related activity component during the early and late epochs in a limited number of cells changed during the trials in which the choice was erroneously made. Second, the choice probability during the late epoch was significant. These results suggest that interval-related V1 activity covaried with interval choice.

4.2. Choice related signal and its correlation with sensory response

In our behavioral task, V1 neurons showed not only the activity component related to discrimination of sequence stimulus, but also the activity component related to behavioral choice. In line with the previous study in orientation discrimination (Nienborg and Cumming, 2014) and saccadic target choice (Palmer et al., 2007), we observed choice probability in V1. The choice probability during interval discrimination task was comparable to the mean CP of 0.54 during orientation discrimination (Nienborg and Cumming, 2014), suggesting that the temporal interval related signal is as strong as stimulus orientation related signal in V1 in terms of correlation with behavioral choice. Intriguing is the observation that the choice related activity component during the choice period appeared a continuation from the activity difference in

sensory period (Figures 12,16). These suggest that the activity fluctuation in sensory response in the identical stimulus condition is maintained as evolving choice signal. This process, however, is not exclusively confined within V1, and may occur interactively among cortical areas, as shown in a curve-tracing task (Khayat et al., 2009).

4.3. Reward related neural activity component in V1

Reward related signals are found nearly all cortical and subcortical structures in human, as revealed with fMRI (Vickery et al. 2011), suggesting their global modulatory roles. Previous report of reward related signals in V1 has focused on reward timing related signal and its origin in rodents (Gavornik and Bear 2014).

We found a clear reward-related activity component in the LFP both in averaged waveform amplitude and in spectral power in the reward period after saccade onset (Figure 32). The significant period was around 350-510 ms of saccade onset in both monkeys. In contrast, reward effect of spike activity was not found in the same period in both animals (Figure 33 C,D). To our knowledge, this is the first to find a reward related activity component in the primate V1. The reward related signal found in the current study is intriguing in a number of aspects. First, unlike previous studies, the activity occurred after the reward, not before as in previous studies. Thus, it is not likely related to its prediction. Second, the signal is in the form of LFP, but subthrehsold to spike initiation. However, subthrehsold LFP is known to influence subsequent spike

activity (Kim et al., 2015). Third, the delivery of reward changed the level of spontaneous activity (Figures 39-41) and visual response (Figures 42-44) in the next trial. This change occurred only for a subset of recording sites, suggesting a selective connectivity from the source. This is consistent with the finding from the study using in vivo two-photon calcium imaging in mouse primary visual cortex (V1) that a non-uniform spatial distribution of reward effects across the cortical surface was observed (Goltstein et al. 2013). Fourth, the reward related signal was stronger in monkey DC who performed better in the task, suggesting that training induced reward-dependent changes in V1 activity during pre-target and post-target periods in the next trial. Finally, the reward was selectively related to the choice behavior in the next trial (Figure 46), the reward related signal may not simply be a modulatory signal for arousal or excitability of cells. Perhaps these results may be interpreted as following. Perceptual decision consists of multiple stages including sensory encoding and motor performance, and in perceptual decision task, reinforcement modifies adaptive strategy based on the statistics of the history of combined choice and reward (Abrahamyan et al. 2016; Barraclough et al. 2004). The reward related signal in V1 may reflect this strategy and calibrate sensory measurements.

4.4. Relation to motion processing

Visual motion information is extracted by detecting the changes of visual features in space and time. We found that the single neurons of monkey primary visual cortex (V1) were sensitive to tens-of-millisecond interval between visual

events across the border of the receptive field. These results indicate that V1 neurons can time tens-of-milliseconds interval based on the receptive field center and surround interaction, and shed lights on how visual motion that extends across the receptive field can be extracted.

A stimulus sequence consisting of two stimuli that are close but not identical in spatial and temporal dimensions invoke apparent motion. The S1-S2 sequence used in the current study induced apparent motion that moved in the direction from the S1 to S2 locations, when we tested ourselves. The motion speed is comparable to the velocity tuning of MT neurons (Movshon and Newsome 1996; Wilson et al. 1992). The temporal interval between spatially-displaced sequential targets and perceived motion speed are closely related to each other, and the SOA then is a determinant of the perceived motion speed. However, it appears that SOA-dependency is not simply related to speed tuning; for a given speed, a doubling of the spatial interval was not accompanied by a doubling of the temporal interval (Kim et al., 2012).

In our experimental condition, S1 does not evoke spike activity at recording sites. However, it evokes subthreshold local field potential at the recording site and modulate spike activity in response to S2 (Kim et al. 2015). From theoretical perspectives, the subthreshold local field potential provides a physiological mechanism for a cross-linkage in motion detectors such as the Reichardt detector (van Santen and Sperling 1985).

The interval-related activity component suggests that V1 neurons are sensitive to the speed of global motion, likely supplementing speed selectivity for local motion of direction-selective V1 neurons (Orban et al. 1986; Priebe

and Ferster 2005). This is consistent with an increase in response specificity and reliability (Vinje and Gallant 2000) and the idea on the potential role for motion perception (Series et al. 2003) with stimulation of RF surround and potential role of end-stopped V1 neurons for overcoming the aperture problem (Marr 1982) by responding only to the endpoints of long contours (Pack et al. 2003).

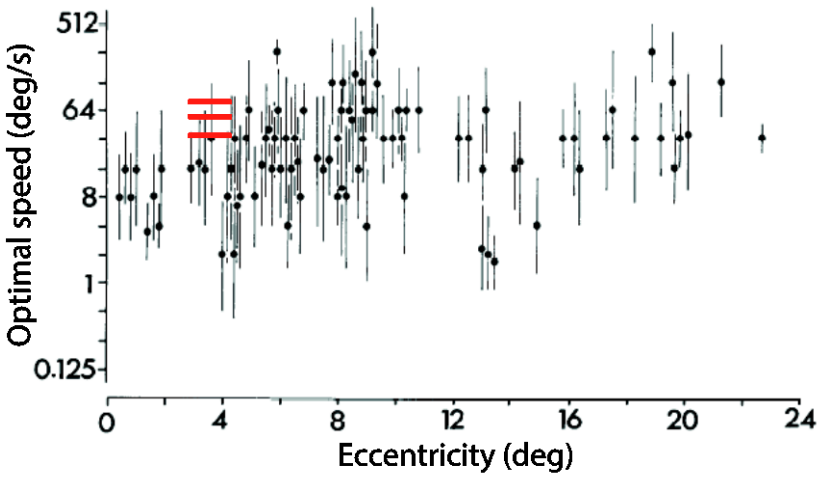

Figure 47. Tuning of motion speed in MT cells, taken from Maunsell and Van Essen (1983). Red bars indicate the speeds of apparent motion formed by the SOAs of 30, 50, and 70 ms and typical spatial separation between S1 and S2.

References

Abrahamyan A, Silva LL, Dakin SC, Carandini M, Gardner JL (2016) Adaptable history biases in human perceptual decisions. Proc Natl Acad Sci U S A 113:E3548-3557.

Ahmed B, Hanazawa A, Undeman C, Eriksson D, Valentiniene S, Roland PE (2008) Cortical dynamics subserving visual apparent motion. Cereb Cortex 18:2796-2810.

Allman J, Miezin F, McGuinness E (1985) Stimulus specific responses from beyond the classical receptive field: neurophysiological mechanisms for local-global comparisons in visual neurons. Ann Rev Neurosci 8:407-430.

Angelucci A, Bressloff PC (2006) Contribution of feedforward, lateral and feedback connections to the classical receptive field center and extra-classical receptive field surround of primate V1 neurons. Prog Brain Res 154:93-120.

Bair W, Cavanaugh JR, Movshon JA (2003) Time course and time-distance relationships for surround suppression in macaque V1 neurons. J Neurosci 23:7690-7701.

Barraclough DJ, Conroy ML, and Lee D. Prefrontal cortex and decision making

in a mixed-strategy game. Nat Neurosci 7: 404-410, 2004.

Bieszczad KM, Weinberger NM (2012) Extinction reveals that primary sensory cortex predicts reinforcement outcome. Eur J Neurosci 35:598-613.

Borst A, Euler T (2011) Seeing things in motion: models, circuits, and mechanisms. Neuron 71:974-994.

Bradley DC, Goyal MS (2008) Velocity computation in the primate visual system. Nat Rev Neurosci 9:686-695.

Britten KH, Newsome WT, Shadlen MN, Celebrini S, Movshon JA (1996) A relationship between behavioral choice and the visual responses of neurons in macaque MT. Vis Neurosci 13:87-100.

Buonomano DV (2003) Timing of neural responses in cortical organotypic slices. Proc Natl Acad Sci U S A 100:4897-4902.

Burt P, Sperling G (1981) Time, distance, and feature trade-offs in visual apparent motion. Psychol Rev 88:171-195.

Chubykin, A. A., Roach, E. B., Bear, M. F., & Shuler, M. G. (2013). A cholinergic mechanism for reward timing within primary visual cortex. *Neuron, 77*(4), 723-735.

Exner S (1888) Einige beobachtungen uber bewegungsnachbilder. Centr Physiol 1:135-140.

Gavornik JP, and Bear MF. Learned spatiotemporal sequence recognition and prediction in primary visual cortex. Nat Neurosci 17: 732-737, 2014.

Geisler WS, Albrecht DG, Crane AM, Stern L (2001) Motion direction signals in the primary visual cortex of cat and monkey. Vis Neurosci 18:501-516.

Gepshtein S, Kubovy M (2007) The lawful perception of apparent motion. J Vis 7:1-15.

Gilroy LA, Hock HS (2009) Simultaneity and sequence in the perception of apparent motion. Atten Percept Psychophys 71:1563-1575.

Goel A, Buonomano DV (2014) Timing as an intrinsic property of neural networks: evidence from in vivo and in vitro experiments. Philos Trans R Soc B 369:20120460.

Goltstein, P. M., Coffey, E. B., Roelfsema, P. R., & Pennartz, C. M. (2013). In vivo two-photon Ca2+ imaging reveals selective reward effects on stimulus-specific assemblies in mouse visual cortex. *The Journal of neuroscience : the official journal of the Society for Neuroscience, 33*(28), 11540-11555.

Grinvald A, Lieke EE, Frostig RD, Hildesheim R (1994) Cortical point-spread function and long-range lateral interactions revealed by real-time optical imaging of macaque monkey primary visual cortex. J Neurosci 14:2545-2568.

Haefner RM, Gerwinn S, Macke JH, Bethge M (2013) Inferring decoding strategies from choice probabilities in the presence of correlated variability. Nat Neurosci 16:235-242.

Hafed ZM, Lovejoy LP, Krauzlis RJ (2011) Modulation of microsaccades in monkey during a covert visual attention task. J Neurosci 31:15219-15230.

Hedges JH, Gartshteyn Y, Kohn A, Rust NC, Shadlen MN, Newsome WT, Movshon JA (2011) Dissociation of neuronal and psychophysical responses to local and global motion. Curr Biol 21:2023-2028.

Hochberg Y, Benjamini Y (1990) More powerful procedures for multiple significance testing. Stat Med 9:811-818.

Huertas MA, Hussain Shuler MG, Shouval HZ (2015) A Simple Network Architecture Accounts for Diverse Reward Time Responses in Primary Visual Cortex. J Neurosci 35:12659-12672.

Khayat PS, Pooresmaeili A, Roelfsema PR (2009) Time course of attentional

modulation in the frontal eye field during curve tracing. J Neurophysiol 101:1813-1822.

Kim K, Kim T, Yoon T, Lee C (2015) Covariation between Spike and LFP Modulations Revealed with Focal and Asynchronous Stimulation of Receptive Field Surround in Monkey Primary Visual Cortex. PLoS ONE 10:e0144929.

Kim T, Kim HR, Kim K, Lee C (2012) Modulation of v1 spike response by temporal interval of spatiotemporal stimulus sequence. PLoS ONE 7:e47543.

Kondo H, and Komatsu H. Suppression on neuronal responses by a metacontrast masking stimulus in monkey V4. Neurosci Res 36: 27-33, 2000.

Lee J, Kim HR, Lee C (2010) Trial-to-trial variability of spike response of V1 and saccadic response time. J Neurophysiol 104:2556-2572.

Liu, C. H., Coleman, J. E., Davoudi, H., Zhang, K., & Hussain Shuler, M. G. (2015). Selective activation of a putative reinforcement signal conditions cued interval timing in primary visual cortex. *Current biology : CB, 25*(12), 1551-1561.

Liston DB, Stone LS (2008) Effects of prior information and reward on oculomotor and perceptual choices. J Neurosci 28:13866-13875.

Marr D (1982) Vision. San Francisco: W.H. Freeman.

Mauk MD, Buonomano DV (2004) The neural basis of temporal processing. Ann Rev Neurosci 27:307-340.

Maunsell JH, Van Essen DC (1983) Functional properties of neurons in middle temporal visual area of the macaque monkey. I. Selectivity for stimulus direction, speed, and orientation. J Neurophysiol 49:1127-1147.

Mayo JP, Sommer MA (2013) Neuronal correlates of visual time perception at brief timescales. PNAS 110:1506-1511.

McIlwain JT (1975) Visual receptive fields and their images in superior colliculus of the cat. J Neurophysiol 38:219-230.

Mizobe K, Polat U, Pettet MW, Kasamatsu T (2001) Facilitation and suppression of single striate-cell activity by spatially discrete pattern stimuli presented beyond the receptive field. Vis Neurosci 18:377-391.

Movshon JA, Newsome WT (1996) Visual response properties of striate cortical neurons projecting to area MT in macaque monkeys. J Neurosci 16:7733-7741.

Movshon JA. Dissociation of neuronal and psychophysical responses to local

and global motion. Curr Biol 21: 2023-2028, 2011.

Muller JR, Metha AB, Krauskopf J, Lennie P (2003) Local signals from beyond the receptive fields of striate cortical neurons. J Neurophysiol 90:822-831.

Newsome WT, Mikami A, Wurtz RH (1986) Motion selectivity in macaque visual cortex. III. Psychophysics and physiology of apparent motion. J Neurophysiol 55:1340-1351.

Nienborg H, Cumming BG (2009) Decision-related activity in sensory neurons reflects more than a neuron's causal effect. Nature 459:89-92.

Nienborg H, Cumming BG (2014) Decision-related activity in sensory neurons may depend on the columnar architecture of cerebral cortex. J Neurosci 34:3579-3585.

Nienborg H, Cohen MR, Cumming BG (2012) Decision-related activity in sensory neurons: correlations among neurons and with behavior. Ann Rev Neurosci 35:463-483.

Nienborg H, and Cumming BG. Decision-related activity in sensory neurons may depend on the columnar architecture of cerebral cortex. J Neurosci 34: 3579-3585, 2014.

Nortmann N, Rekauzke S, Onat S, Konig P, Jancke D (2013) Primary Visual Cortex Represents the Difference Between Past and Present. Cereb Cortex.

Orban GA, Kennedy H, Bullier J (1986) Velocity sensitivity and direction selectivity of neurons in areas V1 and V2 of the monkey: influence of eccentricity. J Neurophysiol 56:462-480.

Pack CC, Livingstone MS, Duffy KR, Born RT (2003) End-stopping and the aperture problem: two-dimensional motion signals in macaque V1. Neuron 39:671-680.

Palmer C, Cheng SY, Seidemann E (2007) Linking neuronal and behavioral performance in a reaction-time visual detection task. J Neurosci 27:8122-8137.

Paradis AL, Morel S, Series P, Lorenceau J (2012) Speeding up the brain: when spatial facilitation translates into latency shortening. Front Hum Neurosci 6:330.

Poort J, Raudies F, Wannig A, Lamme VA, Neumann H, Roelfsema PR (2012) The role of attention in figure-ground segregation in areas V1 and V4 of the visual cortex. Neuron 75:143-156.

Priebe NJ, Ferster D (2005) Direction selectivity of excitation and inhibition in simple cells of the cat primary visual cortex. Neuron 45:133-145.

Reichardt W (1961) Autocorrelation, a principle for the evaluation of sensory information by the central nervous system. In: Sensory communication (Rosenblith W, ed), pp 303–317. New York: Wiley.

Rorie AE, Gao J, McClelland JL, Newsome WT (2010) Integration of sensory and reward information during perceptual decision-making in lateral intraparietal cortex (LIP) of the macaque monkey. PLoS ONE 5:e9308.

Sayer, R. J., Friedlander, M. J., & Redman, S. J. (1990). The time course and amplitude of EPSPs evoked at synapses between pairs of CA3/CA1 neurons in the hippocampal slice. *The Journal of neuroscience*

Sceniak MP, Ringach DL, Hawken MJ, Shapley R (1999) Contrast's effect on spatial summation by macaque V1 neurons. Nat Neurosci 2:733-739.

Schiller PH, and Smith MC. Detection in metacontrast. J Exp Psychol 71: 32-39, 1966.

Schwartz O, Hsu A, Dayan P (2007) Space and time in visual context. Nat Rev Neurosci 8:522-535.

Series P, Lorenceau J, Fregnac Y (2003) The "silent" surround of V1 receptive fields: theory and experiments. J Physiol Paris 97:453-474.

Shadlen MN, Britten KH, Newsome WT, Movshon JA (1996) A computational analysis of the relationship between neuronal and behavioral responses to visual motion. J Neurosci 16:1486-1510.

Shuler, M. G., & Bear, M. F. (2006). Reward timing in the primary visual cortex. *Science, 311*(5767), 1606-1609

Silverstein DN. A computational investigation of feedforward and feedback processing in metacontrast backward masking. Front Psychol 6: 6, 2015.

Stanisor L, van der Togt C, Pennartz CM, Roelfsema PR (2013) A unified selection signal for attention and reward in primary visual cortex. Proc Natl Acad Sci U S A 110:9136-9141.

Thompson KG, Hanes DP, Bichot NP, Schall JD (1996) Perceptual and motor processing stages identified in the activity of macaque frontal eye field neurons during visual search. J Neurophysiol 76:4040-4055.

van Rossum, M. C. (2001). A novel spike distance. Neural Computation, 13(4), 751-763.

van Santen JP, Sperling G (1985) Elaborated Reichardt detectors. J Opt Soc Amer 2:300-321.

Vickery TJ, Chun MM, Lee D (2011) Ubiquity and specificity of reinforcement signals throughout the human brain. Neuron 72:166-177.

Vinje WE, Gallant JL (2000) Sparse coding and decorrelation in primary visual cortex during natural vision. Science 287:1273-1276.

Wilson HR, Ferrera VP, Yo C (1992) A psychophysically motivated model for two-dimensional motion perception. Vis Neurosci 9:79-97.

국문초록

수십분의 일초 시간의 시각변별 과제에서 원숭이 일차시각피질의 신경 활동

서울대학교 대학원
협동과정 인지과학 전공
윤태환

물체의 운동과 같은 시각적 이벤트를 변별하기 위해서는 시간에 대한 정보처리가 필수적이다. 하지만, 동물이 시각적으로 운동을 인식하는데 수십분의 일초의 시간 단위는 매우 중요함에도 그것이 어떻게 두뇌에서 처리되는지에 대해서는 그다지 알려진 것이 없다.

본 논문에서는 레서스 원숭이에게 두 개의 정지 시각 자극이 수십분의 일초 간격을 두고 순차적으로 제시될 때 일차시각피질의 신경세포가 그 시간 간격에 따라 활동 수준이 달라지는 것을 밝혔다. 이때 첫 번째 자극은 관찰하고 있는 세포의 수용장(receptive field)의 바깥에, 두 번째 자극은 세포의 수용장에 제시되었다. 더해서, 자극 간의 시간 간격의 길고 짧음을 훈련 받은 원숭이가 자극을 변별하는 실험을 하는 동안에 일차시각피질의 신경 세포에서 다른 두 가지 세포의 활동 요소를 발견하였다. 첫째는 동물이 곧 결정할 선택 행동에 따라 그 크기가 변화하는

신경 반응으로 선택 확률이 (choice probability) 일차시각피질 신경 세포의 각도 변별의 그것에 상당한 크기였다. 또, 국소 전위장 (local field potential) 에서 동물에게 주어지는 보상에 따라 그 크기가 변화하는 신경 반응 요소였다.

이러한 결과는 일차시각피질의 신경 세포가 수십분의 일초의 시간 간격에 선택적으로 활동이 변화하고 또, 세포의 반응 크기가 제시 되는 자극과 별도로 시간 간격 변별의 판단에 따라 조절됨을 보여준다. 이것은 시간 간격에 대한 시각변별 과제를 수행할 때 일차시각피질에서 center-surround interaction가 새로운 기능적 역할을 가지고 있음을 시사하는 결과이다.

주요어 : 일차시각피질, 시간 간격 변별, 단일 신경 세포 활동 측정, 국소장 전위, 선택 확률, 원숭이

학 번 : 2006-30743